



5-1997

Debris Slide Susceptibility Analysis in the Mount Leconte-Newfound Gap Area of the Great Smoky Mountains, Tennessee and North Carolina

Joseph P. Henderson
University of Tennessee - Knoxville

Recommended Citation

Henderson, Joseph P., "Debris Slide Susceptibility Analysis in the Mount Leconte-Newfound Gap Area of the Great Smoky Mountains, Tennessee and North Carolina." Master's Thesis, University of Tennessee, 1997.
https://trace.tennessee.edu/utk_gradthes/1440

This Thesis is brought to you for free and open access by the Graduate School at Trace: Tennessee Research and Creative Exchange. It has been accepted for inclusion in Masters Theses by an authorized administrator of Trace: Tennessee Research and Creative Exchange. For more information, please contact trace@utk.edu.

To the Graduate Council:

I am submitting herewith a thesis written by Joseph P. Henderson entitled "Debris Slide Susceptibility Analysis in the Mount Leconte-Newfound Gap Area of the Great Smoky Mountains, Tennessee and North Carolina." I have examined the final electronic copy of this thesis for form and content and recommend that it be accepted in partial fulfillment of the requirements for the degree of Master of Science, with a major in Geography.

Carol P. Harden, Major Professor

We have read this thesis and recommend its acceptance:

John Rehder, Bob Muenchen

Accepted for the Council:

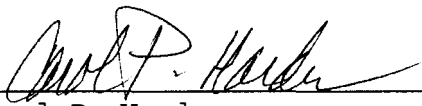
Dixie L. Thompson

Vice Provost and Dean of the Graduate School

(Original signatures are on file with official student records.)


To the Graduate Council:

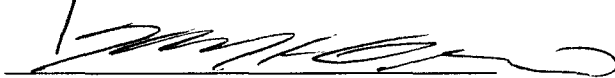
I am submitting herewith a thesis written by Joseph P. Henderson entitled "Debris Slide Susceptibility Analysis in the Mount Leconte-Newfound Gap Area of the Great Smoky Mountains, Tennessee and North Carolina." I have examined the final copy of this thesis for form and content and recommend that it be accepted in partial fulfillment of the requirements for the degree of Master of Science, with a major in Geography.




Carol P. Harden,
Major Professor

We have read this thesis
and recommend its acceptance:





Accepted for the Council:



Associate Vice Chancellor and
Dean of the Graduate School

DEBRIS SLIDE SUSCEPTIBILITY ANALYSIS
IN THE MOUNT LECONTE-NEWFOUND GAP AREA OF THE
GREAT SMOKY MOUNTAINS, TENNESSEE AND NORTH CAROLINA

A Thesis
Presented for the
Master of Science
Degree
The University of Tennessee, Knoxville

Joseph P. Henderson

May 1997

DEDICATION

This thesis is dedicated to my parents .

Mr. Curtis E. Henderson

and

Mrs. Jean B. Henderson

for their love, support, and guidance.

ACKNOWLEDGMENTS

I wish to express my sincere gratitude to all who assisted in the completion of this project. I want to especially thank my committee chair, Dr. Carol Harden, for her expert guidance and encouragement. I also thank Mr. Bob Muenchen for his assistance with statistical analysis. I am also grateful for the advice and assistance of Dr. Ken Orvis, Dr. John Rehder and Dr. Bruce Ralston of the Geography Department faculty and Mr. Roger Tankersley, fellow graduate student.

Thanks are extended to the staff at the Great Smoky Mountains Twin Creeks Research Laboratory in Gatlinburg, especially Michael Kunze and Charles Parker. Grateful acknowledgment is made to Mr. Karl Hermann for his technical assistance with the Southern Appalachian Assessment GIS data base. Additionally, I wish to sincerely thank the United States Army and the Department of Geography at the University of Tennessee Knoxville for this educational opportunity. Special thanks are extended to LTC (Retired) William Doe, former Professor in the Department of Geography and Environmental Engineering at the United States Military Academy, for his "long-range" mentoring and encouragement.

Finally, and most importantly, I am forever grateful to my wife, Kye Hwa, for her patience and understanding. And to my daughters, Rose, and Suzie, for keeping Daddy motivated.

ABSTRACT

In this study, Geographic Information System (GIS) techniques are combined with statistical analyses to create two debris slide susceptibility maps of the Mount Leconte-Newfound Gap area in the Great Smoky Mountains National Park (GRSMNP). This area has experienced numerous debris slide events in the past half century. Although the area has been the subject of several mass movement studies, this is the first known application of debris slide susceptibility mapping in the GRSMNP.

The factors that influence the potential for slope failure are extremely variable, and the interrelationships between these factors are complex. Six topographic variables (slope angle, slope aspect, slope form (plan and profile), geology, distance to ridge crest, and precipitation) were examined to determine their influence on slope stability. Results indicate that slope angles in the 35-40 degree range are the most susceptible to failure. Among slope aspects, south facing slopes are most failure-prone. Slopes that are concave in cross section are more susceptible than other slope forms. The rock type with the highest degree of susceptibility is the Anakeesta Formation. Locations that are slightly below the ridge crest have the highest incidences of failure. Lastly, susceptibility tends to increase with the amount of precipitation received.

The two statistical techniques used to produce the debris slide susceptibility maps were failure rate analysis and logistic regression. I found that logistic regression is a superior method because scalar values are used rather than categorical values so that a greater amount of information is retained. This type of slope failure analysis over a broad area provides important information to planners and demonstrates the utility of GIS in debris slide susceptibility mapping.

TABLE OF CONTENTS

CHAPTER	PAGE
I. INTRODUCTION	1
Purpose of Study	2
II. DEBRIS SLIDES	4
Definition and Geomorphic Significance	4
Causes	7
Approaches to Landslide Susceptibility Studies	8
III. GIS AND DEM FUNDAMENTALS	13
GIS Fundamentals	13
DEM Fundamentals	17
IV. THE STUDY AREA	21
Location	21
Relief and Drainage	22
Geology	22
Structure	26
Surficial Material	28
Vegetation	29
Climate and Weather	30
Anthropogenic Influence	31
Previous Studies	32
Historical Slide Activity	33
V. METHODS AND TOOLS	37
Data Sources	37
Variable Selection	39
Slope Angle	39
Slope Aspect	40
Slope Form	42
Lithology	44
Distance from Ridge Crest	45
Precipitation	45
Existing Slides	48
Variables Not Considered	49
Hardware/Software Tools	50
Analysis Techniques	50
Failure Rate Analysis	50
Logistic Regression	62
VI. RESULTS AND DISCUSSION	66
Failure Rate Analysis	66
Slope Angle	68
Slope Aspect	71
Slope Form	73
Lithology	80
Distance from Ridge Crest	82
Precipitation	84
Debris Slide Susceptibility Map	87

CHAPTER	PAGE
Logistic Regression Analysis	90
Debris Slide Susceptibility Map	94
Comparison of Methods and Resulting Maps	96
Limitations of Debris Slide Susceptibility Maps	100
VII. SUMMARY AND CONCLUSIONS	103
LIST OF REFERENCES	108
APPENDICES	117
APPENDIX A. Computer Algorithms	118
APPENDIX B. Azimuth Calculations	123
VITA	124

LIST OF TABLES

TABLE	PAGE
1. Debris Slide History	33
2. Failure Rate Variables and Classes	53
3. Ranking of Attribute Classes by Failure Rate	67
4. Failure Rate Susceptibility Map Results	87
5. Logistic Regression Statistics for Key Variables	93
6. Logistic Regression Susceptibility Map Results	94

LIST OF FIGURES

FIGURE	PAGE
1. Diagram of Debris Slide Elements	6
2. The Overlay Concept in Geographic Information Systems ..	16
3. Example of Distortion in Raster Format	18
4. Location Map of the Study Area	23
5. Geologic Map of the Study Area	25
6. Outcrop of the Anakeesta Formation	27
7. Backwasting of Debris Slide Scars on Anakeesta Ridge	34
8. Map of Precipitation Gauge Locations	47
9. Map of Debris Slide Locations	51
10. Map of Slope Angle Classes	54
11. Map of Slope Aspect Classes	55
12. Map of Slope Plan Form Classes	56
13. Map of Slope Profile Form Classes	57
14. Geological Formations in the Study Area	58
15. Map of Distance from Ridge Crest Classes	59
16. Map of Annual Precipitation as Extrapolated from Data of Smallshaw (1953)	60
17. Relative Frequency and Failure Rate for Slope Angle	69
18. Relative Frequency and Failure Rate for Slope Aspect ...	72
19. Relative Frequency and Failure Rate for Slope Plan Form	74
20. Relative Frequency and Failure Rate for Slope Profile Form	75
21. Wedge Failure on Anakeesta Ridge	77
22. Relative Frequency and Failure Rate for Slope Form	79
23. Relative Frequency and Failure Rate for Lithology	81

FIGURE	PAGE
24. Relative Frequency and Failure Rate for Distance from Ridge Crest	83
25. Relative Frequency and Failure Rate for Total Annual Precipitation	85
26. Map of Debris Slide Susceptibility Zones Determined by Failure Rate Analysis	88
27. Map of Debris Slide Susceptibility Determined using Failure Rate Analysis and Printed using Continuous Shading	89
28. Map of Debris Slide Susceptibility Zones Determined by Logistic Regression	95
29. Map of Debris Slide Susceptibility Determined using Logistic Regression and Printed using Continuous Shading	97

CHAPTER I

INTRODUCTION

Debris slides and debris flows occur extensively in the Appalachian Highlands. More than 3,000 slides have been recognized in the region, with over 1,800 occurring in this century alone (Pariseau and Voight, 1979). Debris flows pose a hazard to humans due to inundation and impact from rapidly moving debris, particularly large boulders and trees (Wieczorek, 1984). The human use and settlement of previously underdeveloped mountain regions has increasingly exposed human activities to landslide hazard (Jones, 1992).

Taxpayers are generally unaware of the magnitude of the annual cost of landslide damage, but in the U.S., total annual costs are in excess of \$1 billion (Fleming and Taylor, 1980). Direct effects to mankind include loss of life, damage to natural resources (vegetation, land, and soil), and delay of and damage to development projects like roads and communication lines (Gupta and Joshi, 1990). Despite the magnitude of slide damage, landslides continue to be unrecognized as a major hazard because their impacts are usually local. Many slides occur in such remote locations that their impact does not warrant recording.

A greater understanding of these mass movements by the general public is important as landsliding is one of the most predictable of geological hazards (Jones, 1992). Areas that

experience repeated landsliding episodes can be examined to determine the primary factors contributing to the mass movements. Based on these factors, a landslide susceptibility assessment can be performed that identifies tracts of land with different levels of hazard potential (Jones, 1992).

A variety of methods have been developed to evaluate slope failure susceptibility in an area. One of the more advanced methods for landslide susceptibility analysis over a broad area utilizes computer processing. The computer assisted analysis of factors creates a very powerful method for assessing landslide potential and creating a susceptibility map (Varnes, 1984). Digital elevation models (DEMs) and Geographic Information Systems (GISs) are the primary tools available for computer analysis of the terrain.

Purpose of Study

The purpose of this study is to use Geographic Information Systems and statistical analysis to evaluate landslide hazard susceptibility in an area of the Great Smoky Mountains National Park (GSMNP) that has experienced numerous debris slides during the past half century. Computer assisted techniques will be used to:

- 1) Create a debris slide susceptibility map of the study area.
- 2) Determine the relative importance of various factors in debris slide occurrence.

This study is the first known application of debris slide susceptibility mapping in the National Park. It will examine the

utility of Geographic Information Systems in the study of landslide potential. Furthermore, the research will allow a greater understanding of the slope processes operating in this area of the Great Smoky Mountains. This type of information is important to effective land use planning in mountain environments, as areas most prone to failure can be excluded from development.

This thesis begins with a discussion of the debris slide literature, including definitions and approaches used in other landslide susceptibility studies, to provide a background for debris slide analysis in the study area. This discussion is followed by a brief section on the fundamentals of GISs and DEMs, two important tools in slope stability analysis. Next, I describe the physical nature of the area studied and its recent history of debris slide activity. The fifth chapter outlines the data collection methods and slope failure susceptibility analysis techniques used in this study. Lastly, I discuss the results of the analysis, emphasizing the relative importance of each variable and the merits/deficiencies of the resultant debris slide susceptibility maps.

CHAPTER II

DEBRIS SLIDES

It is important to discuss the pertinent literature on debris slides. This chapter begins with a definition of debris slides, their importance in landscape modification, and their major causes. Next, I present the common approaches to landslide susceptibility studies, describe the approach chosen in this study, and explain why this procedure was employed.

Definition and Geomorphic Significance

Mass movement is the outward or downward gravitational movement of earth material without the aid of running water as a transportational agent (Crozier, 1986). Debris slides are a type of mass movement involving the rapid downhill movement of soil, rocks, trees and other vegetation, and water (Williams and Guy, 1973). Debris flows are distinguished from debris slides by higher water content and continuous internal deformation (Clark, 1987). Sharpe used the term "debris avalanche" to refer to flowing slides in humid regions with a good covering of vegetation (Sharpe, 1938). Almost invariably, they are preceded by heavy rains that increase the weight of the unadjusted material and aid in its lubrication (Sharpe, 1938).

The typical debris slide/flow leaves a characteristic slide scar, a long, relatively narrow track, and occurs on steep mountain

slopes. In many cases, there is no definable subdivision between scar and track, and the combination of these features may be referred to as a chute (Clark, 1987) (Figure 1). The initiating movement is along a discrete surface and may be rotational, translational, or complex (Varnes, 1978). Debris slides become transitional to debris flows in a flow track, possibly related to added water content, topographic constriction, and increasing velocity (Clark, 1987). Debris fans, debris piles, or debris dams are common depositional features found below slide tracks (Hack and Goodlett, 1960).

In the Mount Leconte area, movement in the higher portion of the slide tracks was apparently sliding, whereas flowage was probably the main mechanism in the lower segments (Bogucki, 1970). The mass movements in the study area will be referred to as debris slides for ease of terminology, since sliding evidently initiated the movement. The generic term landslides will be used to describe all varieties of rapid mass movements on slopes to include fall, topple, slide, or flow (Varnes, 1984).

Landslides are among the most important processes of a catastrophic type that lead to modification of surface morphology (Gupta and Joshi, 1990). Debris slides are an important agent in valley formation (Hack and Goodlett, 1960). Many first order hollows may originate, at least in part, by these processes (Ryan and Clark, 1989). The geomorphic effectiveness of these mass movements is due to their ability to erode large quantities of regolith, deepening old channels and eroding new ones. There is

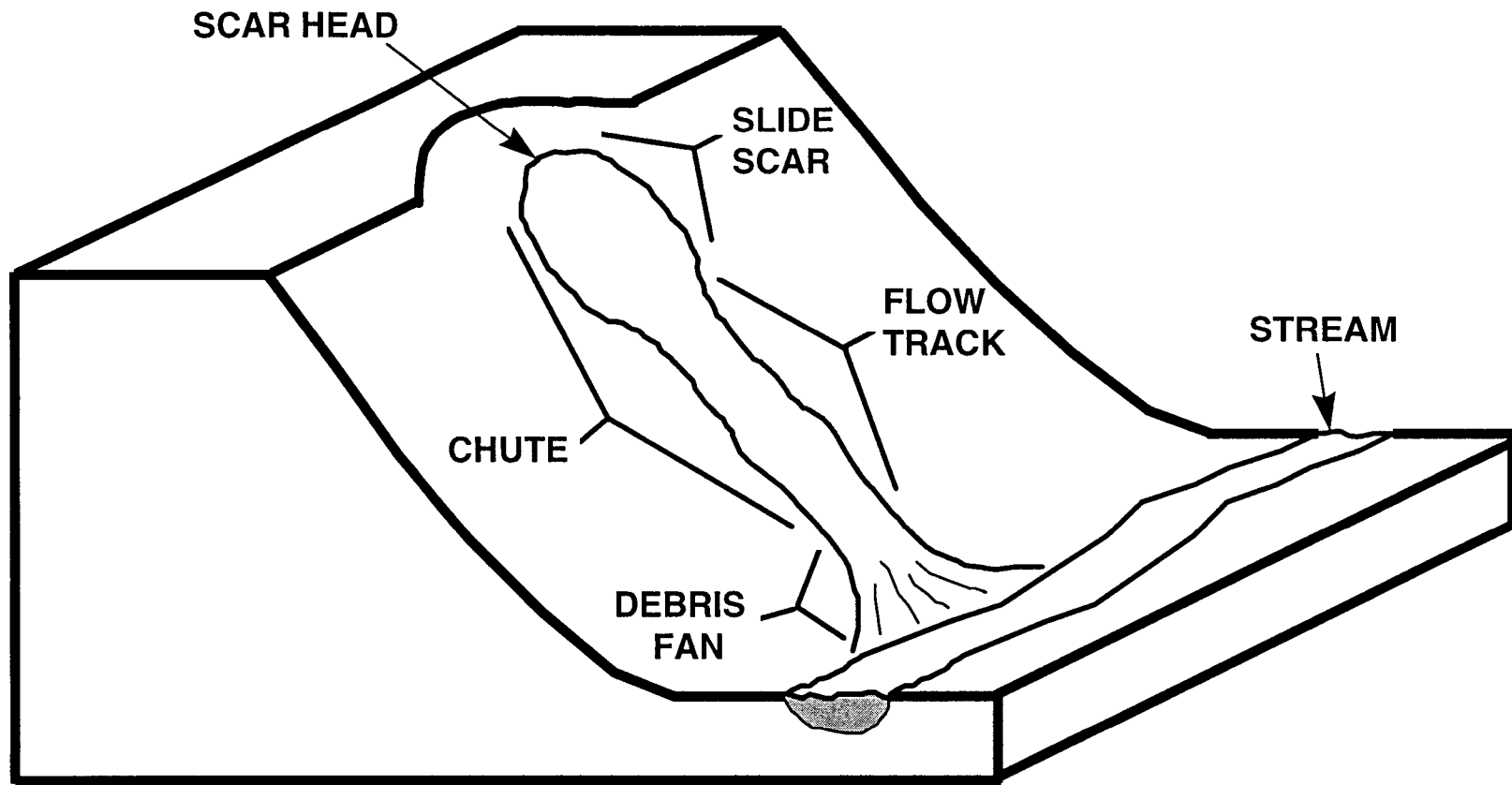


Figure 1. Diagram of Debris Slide Elements. (Source: Clark, 1987)

also a longer recovery time for debris slides than for small scale movements such as slips (Jacobson et al., 1987b).

Causes

Debris sliding in any specific area is the result of the complex interaction of a number of causes that will vary in significance over space and time (Jones, 1992). Although the causes of slides are diverse, the mechanisms are now thought to be reasonably well understood. The major causes in a particular area can be identified and their contributions weighed (Clark et al., 1987).

In all types of slope movement, the slope becomes unstable when the forces acting on the slope exceed the strength of the material that forms the slope. This relationship is represented by the factor of safety (FS) which is the ratio of the shearing strength to the shearing stress. A site where these forces are equal is in equilibrium ($FS = 1$). Where $FS > 1$, the site should be stable, while where $FS < 1$, the site should have failed or at least be unstable (Shasko and Keller, 1991). The stress which exists on all slopes is the force of gravity. However, the magnitude of the downslope component of gravitational stress as well as the shear strength of the material can vary greatly across a landscape, particularly in an area of high relief. The factors which cause the factor of safety to be less than unity on a slope are many and diverse.

Sharpe divides the causes of landslides into two main groups: basic or passive causes and active or initiating causes (Sharpe, 1938). Baird (1990) used this classification scheme in his study of wedge failures in East Tennessee. Passive causes are conditions favorable to sliding that may exist for a long period without any movement occurring (Sharpe, 1938). Crozier called these causes "preparatory factors" that make the slope susceptible to movement without actually initiating it (Crozier, 1986). These conditions include lithology, stratigraphy, structure, and topography. Active causes are the impetus that triggers slides on slopes already under the influence of passive conditions (Sharpe, 1938). Triggering mechanisms include removal of support, overloading, and reduction of friction (Sharpe, 1938).

Approaches to Landslide Susceptibility Studies

The end result of landslide susceptibility studies is to produce a map that shows the spatial division of the earth's surface into areas of different potential for future landslide movement, a process known as zonation (Varnes, 1984; Brabb, 1991). There are several methods available to evaluate slope failure susceptibility in an area. The methodology followed depends on the purpose of the study, the scale of the map to be prepared, and the amount of information that is available for the area concerned (Rengers et al., 1992). The two basic modeling approaches involved in assessing slope stability are deductive and inductive.

In the deductive approach, the physical processes involved are identified and represented by a mathematical formula to provide a simulation of the hazard over the area of interest (Wadge et al., 1993). This approach involves detailed geotechnical analysis of surface and subsurface conditions and ground materials. From these data, slope stability models are developed such as the infinite slope model, the ordinary method of slices, and Spencer's method (Shasko and Keller, 1991).

There are several drawbacks to this type of approach when studying slope stability over a broad area. First, supplying sufficient data to meet the needs of these data-hungry models is difficult (Shasko and Keller, 1991). Furthermore, the parameters measured in the laboratory may not be indicative of the natural state of the rocks, which are in varied states of weathering. The problems are magnified because of the large spatial variability across the landscape in large areas (Mantovani et al., 1996). Lastly, investigators using these methods tend to focus on terrain where landslide paths have occurred while ignoring the surrounding landscape (Gao, 1993).

The alternative approach is known as inductive or empirical. In this procedure, the locations of past debris slide events are identified, and the specific environmental conditions at each location are assessed (Wadge et al., 1993). The intent is to find the critical combination of site conditions that produce slope failure. Multivariate statistical methods can be used to search for site conditions such as degree of slope, bedrock type, and

vegetative cover that correlate well with the past occurrence of landslides (McKean et al., 1991). Once the critical combinations are identified, the relative contribution of each variable is given a semi-quantitative measure and the spatial distribution can be mapped to display areas of relative landslide susceptibility (Varnes, 1984; McKean et al., 1991). Areas are given a probabilistic classification of the relative failure potential of slopes subjected to heavy rain, in that slopes classified as having high susceptibility have a higher chance of failing than those in other classes (Aniya, 1985).

Several basic assumptions must be applied in this inductive approach. The first assumption is that conditions that led to slope instability in the past and the present will apply equally well in the future. The second assumption is that the main conditions that cause landsliding can be identified. The final assumption is that the relative significance of individual factors can be evaluated (Jones, 1992).

The choice of variables to examine is largely guesswork, so the model may only explain a small portion of the hazard variance. Also, the data available for the variables may not have the same values as were present during the slide event (Wadge et al., 1993).

Despite these difficulties, the inductive approach was chosen in this study because it fits more closely the capabilities of Geographic Information Systems (GISs) and is the most common method in landslide susceptibility studies. The deductive approach is more usually associated with simulation models in stand-alone

computer programs rather than as a component of a GIS (Wadge et al., 1993). Too, the deductive approach is more commonly used for investigation of single slides rather than a more broad, regional view.

I chose to use Geographic Information Systems in my analysis because of their unique capabilities in analyzing data. When many variables over a broad area need to be collectively considered, computer processing using Geographic Information Systems provides an efficient platform for managing, manipulating, and displaying spatially-explicit data (Gupta and Joshi, 1990). The computer assisted analysis of factors, combined with the automated plotting of a grid of cells to build a map, creates a very powerful and flexible method in landslide hazard assessment (Varnes, 1984).

One of the first uses of the computer in landslide susceptibility mapping was by Newman et al. (1978) in the San Francisco Bay area. This map was created before the advent of Geographic Information Systems, so the product was relatively basic and generalized with few factors involved. In a more recent work, Jacobson, Cron, and McGeehin (1987b) utilized a GIS to overlay slope failures, topography, land cover, and other variables in slope failure analysis. Carrara et al. (1991) employed GIS and discriminant analysis to evaluate landslide hazard in Central Italy. Gao (1993) described the use of a Digital Elevation Model to determine topographic factors influencing landslide potential in Nelson County, Virginia.

Debris sliding is a complex phenomenon that involves numerous factors; over a broad area, large volumes of data must be analyzed to determine the interrelationships between these factors and debris slide occurrence. Computer analysis is well suited for dealing with large data sets. The following chapter will describe some of the basic concepts concerning GIS and DEMs, and it is primarily provided for the reader who is not familiar with these terms.

CHAPTER III

GIS AND DEM FUNDAMENTALS

In this chapter, I discuss some basic concepts concerning both Geographic Information Systems (GIS) and Digital Elevation Models (DEMs). In the GIS section, I describe both vector and raster formats and explain why raster is more appropriate for this study. The short portion on DEMs includes a discussion of DEM types and shows what sort of topographic information can be derived from a DEM.

GIS Fundamentals

Environmental Systems Research Institute (ESRI) defines a Geographic Information System as an organized collection of computer hardware, software, geographic data, and personnel designed to efficiently capture, store, update, manipulate, analyze, and display all forms of geographically referenced information (ESRI, 1993). Stated more simply, a GIS is a computer system capable of holding and using data describing places on the earth's surface.

The strength of GIS analysis is the ability to link spatially referenced data with geographic information about a particular feature on a map. The spatial data can be stored, retrieved, and analyzed to compute new information about map features (Gupta and Joshi, 1990). This information can be displayed in integrative

ways that are readily comprehensible and visual (Band and Moore, 1991).

Most GISs use the cartographic paradigm in which maps are input, information is combined by overlay analysis, and maps are output. This procedure was traditionally performed in the qualitative sense as a manual approach, with a large amount of human interpretation (Band and Moore, 1995). Computerized maps can be generated in approximately the same time and at less cost than a comparable map compiled manually, with the additional benefits of reducing human drudgery and errors and also creating a database for future use (Varnes, 1984).

Spatial information stored in a GIS has traditionally been represented with a cartographic model in one of two formats: vector and raster (Band and Moore, 1995). The choice of whether to use vector or raster is dependent upon the type of geographic phenomena being represented and the type of modeling to be used (ESRI, 1994).

Vector formats, known as the area-category model, use a node, line, and area model to flexibly distinguish between non-overlapping areas (polygons) (Band and Moore, 1995). Each linear feature is represented as a list of ordered x,y coordinates, and attributes are associated with each feature (ESRI, 1993). This database structure represents features very precisely, so vector structures better address problems in which a feature or object itself is more important than the object's location (ESRI, 1994).

The raster model samples the occurrence of events over a regular, predetermined grid (Band and Moore, 1995). The raster data structure is composed of distinct units called cells, and each cell stores a numeric value (ESRI, 1994). Raster data formats are often preferred in many environmental simulation projects as they more readily lend themselves to a finite difference structure and are more compatible with remote sensing imagery and digital terrain data (Band and Moore, 1995).

The raster data structure was chosen for this study because grid-based data storage is better for representing the locational view of geographic data (ESRI, 1994). Raster is also superior to vector in modeling attributes of locations on the earth's surface and working with multiple data types (ESRI, 1994). The raster format, then, was more appropriate for this study, which required determining the spatial relationships of various attributes that affect landslide distribution.

In the raster format, each cell in a grid has a corresponding value representing a specific attribute. Each grid corresponds to a particular attribute, and this logical set of thematic data is known as a layer. GIS operations can work with these layers by overlaying them, executing mathematical operations and other functions that produce new grids whose cell values incorporate information from all parent layers (Figure 2).

It is important to mention the disadvantages of the raster format. At larger areal extents there is pressure to reduce resolution to increase processing speeds. Resolution decreases as

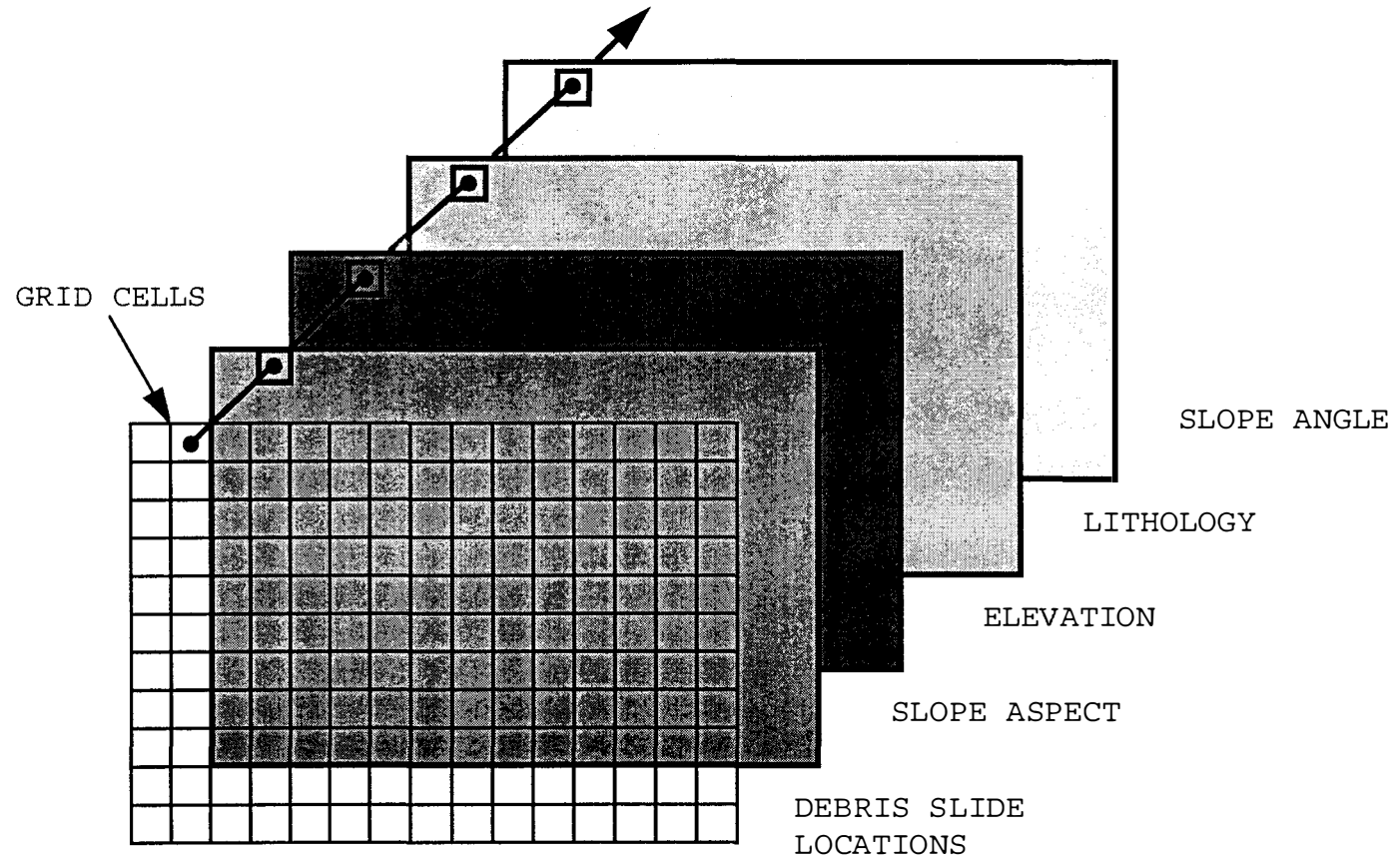


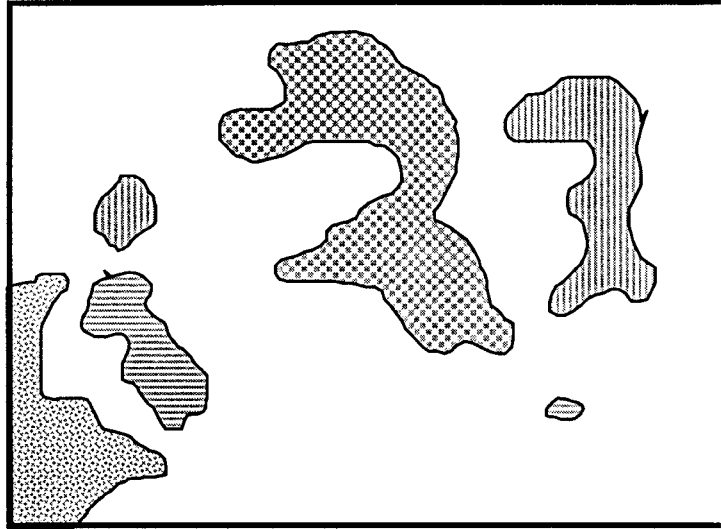
Figure 2. The Overlay Concept in Geographic Information Systems. (Source: Gupta and Joshi, 1990)

the size of grid cells increases. As the resolution decreases, information is lost because larger areas are aggregated into the cell unit area (Band and Moore, 1995). It is critical that the cell size be small enough to capture the required details. In landslide studies, the occurrence of individual mass movements is important input information, and the spatial resolution must be fine enough to allow for their identification (Rengers et al., 1992).

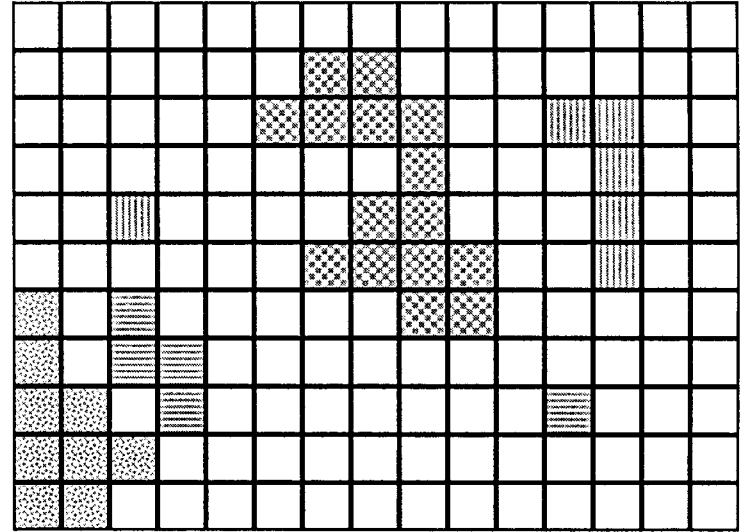
The precision of the individual mass movement shape is also affected by resolution. The cell's unit area must be used to approximate points (single cells), lines (chains of cells), and areas (connected regions) (Band and Moore, 1995). The shape of slides is necessarily deformed by portraying areas with chains or groups of pixels (Figure 3).

DEM Fundamentals

Digital Elevation Models (DEMs) are a subset of Digital Terrain Models, which include all types of digital representations of topographic surfaces (Carter, 1988). Digital Elevation Models consist of a sampled array of elevations for ground positions that are usually, but not always, at regularly spaced intervals (USGS, 1987). Elevation is essentially an instantaneous value, and in most cases, DEM elevations are sampled at discrete points (Franklin, 1987).



Input Map - Polygon
Format



Coarse Resolution Grid - Raster
Format

Figure 3. Example of Distortion in Raster Format.
(Source: ESRI, 1994)

DEMs can be created by digitizing from existing topographic maps, collecting elevations from field surveys, or using photogrammetric stereocompilation (Carter, 1988). Users must generally rely on existing topographic maps or DEMs produced by government agencies because the raw elevation data in the form of stereo photographs or field surveys and the equipment to process these data are not readily available (Moore et al., 1991). When the data and equipment are available, the procedures required to create DEMs are time consuming.

DEMs are produced in three data structures: square-grid, triangulated irregular networks (TINs), and contour-based. The most commonly available data structure is the square-grid network because of the ease of computer implementation and computational efficiency (Moore et al., 1991). Disadvantages to the square-grid format include difficulty in portraying abrupt changes in elevation and loss of information in low resolution grids (Moore et al., 1991). However, the grid-based method was chosen for this study because it is the most efficient structure for estimating topographic attributes and because it interfaces well with other raster-based data layers (Moore et al., 1991).

DEMs can be used to derive a wealth of information about the morphology of a land surface. The types of topographic indices that can be derived from the DEM are slope angle, slope aspect, elevation, and plan/profile curvature (Carter, 1988). GIS analysis of the DEM can also provide surface water routing, site and route selection, and visibility of one place from another (Carter, 1988).

Techniques for determining geomorphic variables from DEMs are generally based on operations in which calculations and decisions are made for a cell based on the values in the eight cells that are spatially adjacent in the raster, known as the "neighborhood" (Jenson and Dominique, 1988). Neighborhood functions may involve addition, identification of highest/lowest value, calculating the mean value of the neighborhood, or more complex operations. Neighborhood operations were used extensively in this analysis and will be discussed in Chapter 5.

This chapter concludes the portion of this paper which is of a general nature. In the chapters that follow, I describe the study area, outline the variables used in the analysis and analysis techniques, and present the results of the research.

CHAPTER IV

THE STUDY AREA

Moving from the general to the specific, I now concentrate on my own work, beginning with the area of study. In this chapter, I provide a general physiographic description of the study area with special emphasis on those aspects that make this area particularly prone to debris slide events. The chapter concludes with a brief history of recent debris slide activity including the latest event triggered by Hurricane Opal.

Location

The study area is located in the Great Smoky Mountains National Park (GSMNP), Tennessee and North Carolina, in the southern section of the Blue Ridge Province. The Blue Ridge Province of the Appalachian Highlands major geomorphic division extends from southern Pennsylvania to northeastern Georgia, a distance of approximately 887 km (550 miles) (Bogucki, 1970). The Great Smoky Mountains lie in eastern Tennessee and western North Carolina between the cities of Knoxville to the west and Asheville to the east. Some of the highest summits in the southeastern United States are found in the national park, with sixteen peaks exceeding 1828 m (6000 ft) above sea level (King and Stupka, 1950).

The study area lies within of the Mt. Leconte and Clingmans Dome 7.5 minute United States Geological Survey quadrangles and

encompasses a 62 km squared area (Figure 4). This site was chosen for its high level of debris slide activity, which has been well documented in previous studies.

Landslide activity in the GSMNP has been most extensive on Mt. Leconte and Anakeesta Ridge. Mount Leconte, with an elevation of 2009 m (6593 ft), is the highest peak in the area and third highest in the GSMNP (Figure 4). Anakeesta Ridge, an east-west trending mountain between Mount Leconte and Newfound Gap, has an average elevation of 1645 m (5400 ft). The ridge is bounded by the second-order Alum Cave Creek to the north and the third-order Walker Camp Prong to the south.

Relief and Drainage

The area is characterized by high relief and steep slopes. Elevations range from a minimum of 787 m to 2009 m (2582 ft to 6593 ft) at the highest point. The slopes are generally very steep, with the majority of slopes in the range of 31-35 degrees. Styx Branch, Trout Branch and Alum Cave Creek are the major streams on the south side of Mt. Leconte.

Geology

The rocks in the Great Smoky Mountains consist of a large mass of pebbly, sandy, and muddy metasedimentary rocks in various stages of metamorphism. Most were formed during some part of the later

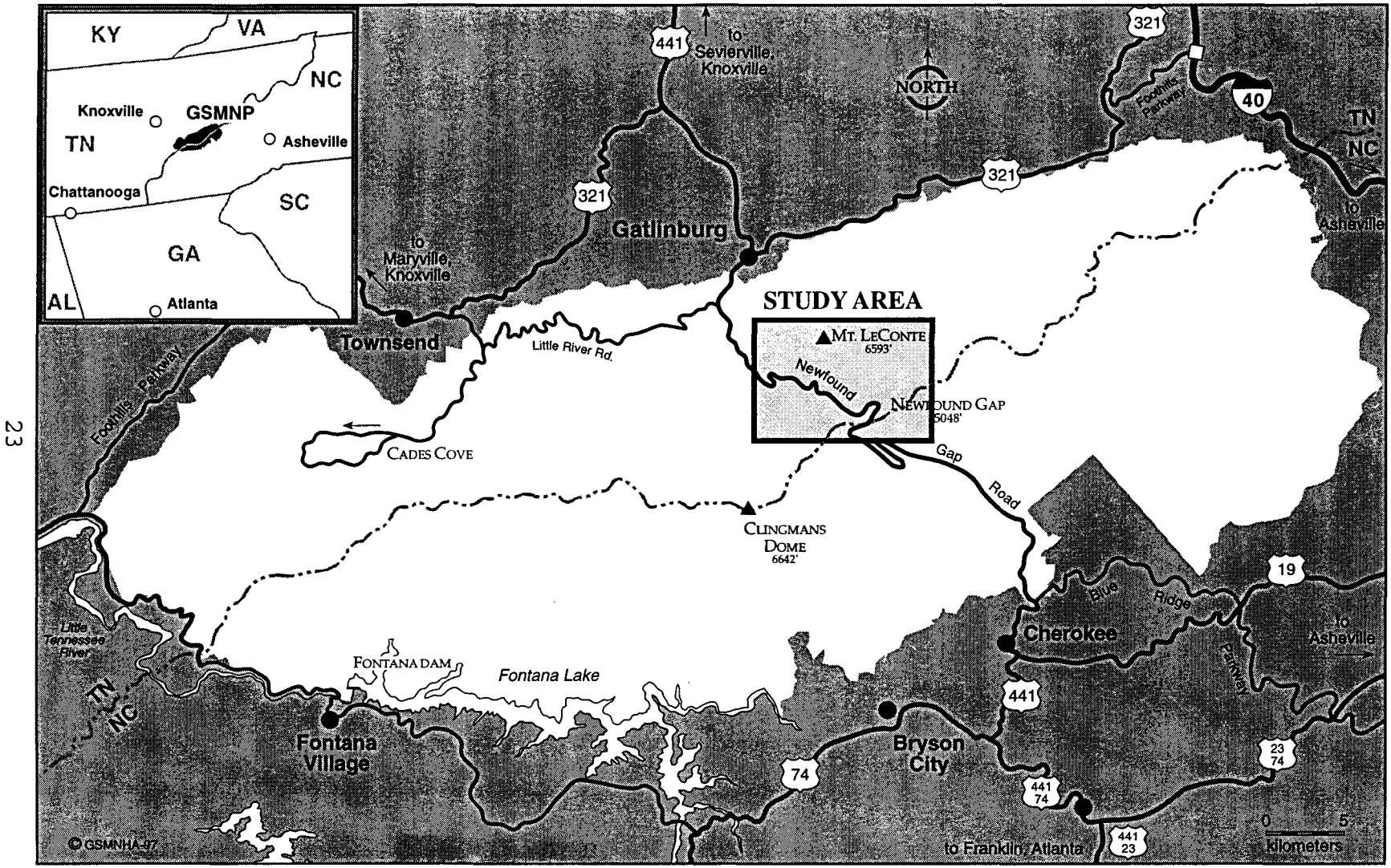


Figure 4. Location Map of the Study Area. (Source: Great Smoky Mountains Natural History Association)

Precambrian time and belong to the Ocoee Series (King et al., 1968). The Ocoee Series overlies a basement complex of granite and metasedimentary gneiss of Precambrian age (Moore, 1988).

The Ocoee Series extends far beyond the Great Smoky Mountains to the northeast and southwest, encompassing a distance of more than 282 km (175 miles) (King et al., 1968). This formation, which covers the entire study area, has been complexly folded and faulted internally and metamorphosed to varying degrees by heat and pressure (King et al., 1968). The lithology consists of sandstones, shales, slates, phyllite, and schist.

The Ocoee Series has three subdivisions: the Snowbird, Great Smoky, and Walden Creek Groups, each separated from the others by major thrust faults (King et al., 1958). The Great Smoky Group, the southernmost sequence of the Ocoee Series, underlies most of the study area and forms the main bulk of the Great Smoky Mountains (King et al., 1968). This group is divided into three intertonguing formations: fine grained Elkmont Sandstone below, coarse grained Thunderhead Sandstone in the middle, and the dark silty and argillaceous rocks of the Anakeesta Formation above (King et al., 1968) (Figure 5).

The two dominant rock types in the study area are Thunderhead Sandstone (52 percent of the area) and the Anakeesta formation (47 percent of the area). These are also the two most abundant formations of the Ocoee Series in the park as a whole (Moore, 1988).

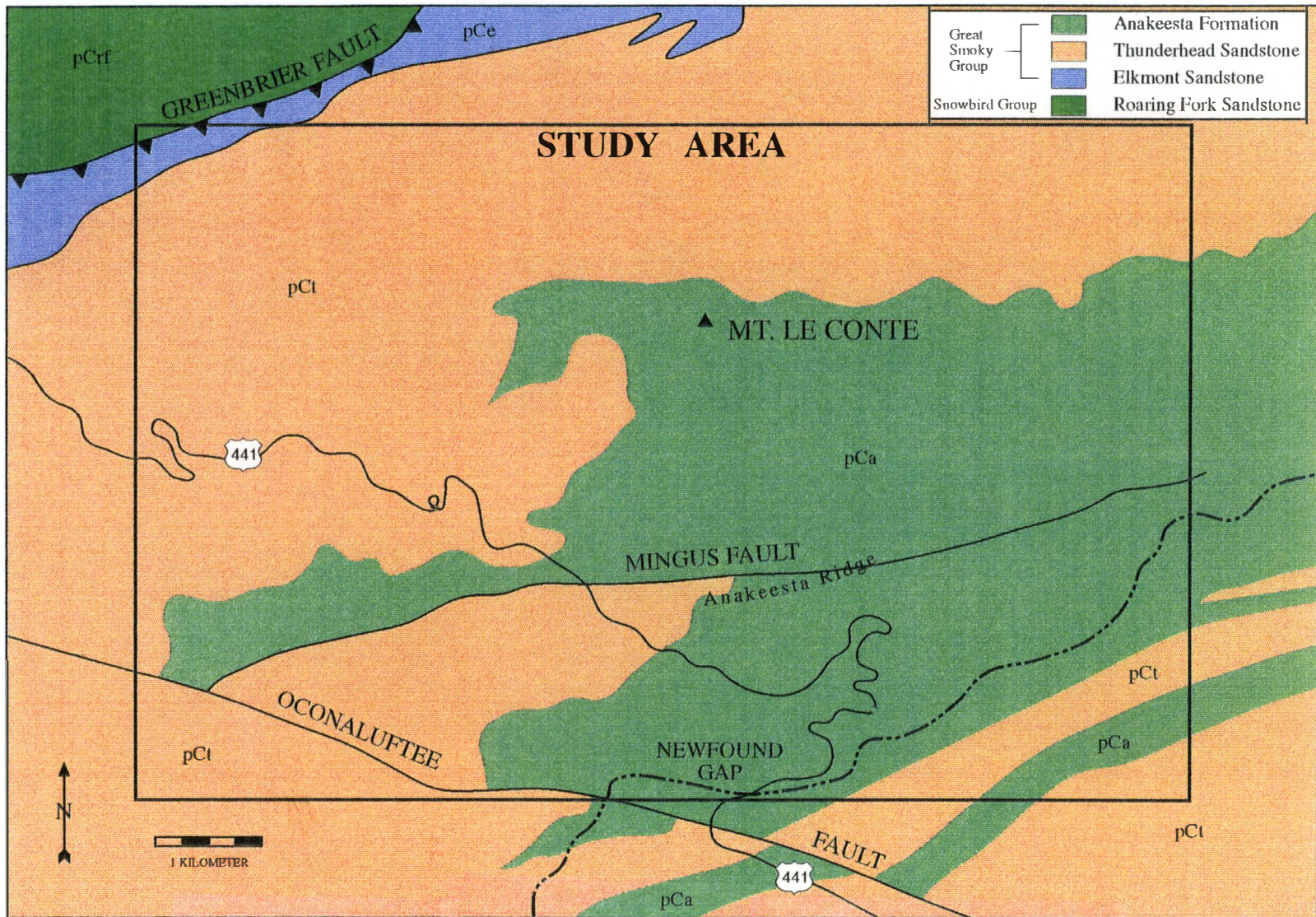


Figure 5. Geologic Map of the Study Area. (Source: King, Neuman, and Hadley, 1968)

Thickest and most widespread is the Thunderhead Sandstone. The Thunderhead Sandstone consists mostly of feldspathic sandstone and fine arkosic conglomerate and includes gray slate, phyllite, quartz mica schist, granite and quartzite conglomerate (Hadley and Goldsmith, 1963). At Mount Leconte, the Thunderhead Sandstone's thickness reaches 1524-1829 m (5000-6000 ft) (King et al., 1958).

The Anakeesta Formation, named for Anakeesta Ridge, intertongues extensively with the Thunderhead Sandstone (King et al., 1968). It includes a variety of rock types such as arkosic pebble conglomerate, graywacke, feldspathic sandstone, chloritoidal slate and argillite, carbonaceous slate, and phyllite (Hadley and Goldsmith, 1963). Individual tongues of this formation do not exceed 610 m (2000 ft) in thickness, but range throughout a stratigraphic sequence of nearly 1524 m (5000 ft) (King et al., 1958). Outcrops of this formation are characterized by narrow, steep sided ridges and craggy pinnacles (King et al., 1958). Abundant bedding, joint, and cleavage discontinuities are present in the Anakeesta formation, providing ample failure planes for slope movement (Clark et al., 1987) (Figure 6).

Structure

The bedrock has undergone extensive folding, faulting, and metamorphosis. There are a number of faults in the Great Smoky Mountains that have a major role in the structural arrangement of the bedrock (Moore, 1988).



Figure 6. Outcrop of the Anakeesta Formation.

Within the study area, one major fault and two minor faults are present (Figure 5). The Greenbrier fault, one of the three major faults in the Great Smoky Mountains, is located just north of the study area; this low angle thrust fault forms the contact between the Great Smoky Group and underlying Snowbird Group of the Ocoee Series. The Mingus fault is a steep reverse fault trending east-west immediately north of Anakeesta Ridge (Hadley and Goldsmith, 1963). The Oconaluftee fault, a right lateral fault trending northwest-southeast, is found 2.5 km southwest of Anakeesta Ridge, and displaces the lower tongue of the Anakeesta Formation approximately 0.8 km (Ryan, 1989). The strike is generally northeast-southwest with dip to the southeast at angles ranging from 26 to 55 degrees (Bogucki, 1970).

Surficial Material

The slopes are mantled with colluvium and fresh or slightly weathered bedrock (Feldkamp, 1984). Within debris slide areas the colluvium is generally deeper on more shallow slopes (Bogucki, 1970). Very little saprolite is present and alluvium is limited to the stream beds or stream edges (Feldkamp, 1984).

Dominant soil types in the high elevations of the GSMNP are Inceptisols of the Umbric Dystrochrept Subgroup, with some Spodosols present on crests of higher domes or peaks under spruce-fir vegetation (Wolfe, 1967). Inceptisols dominate because the steepness of the slopes hinders horizon development.

The Soil Survey of Sevier County, Tennessee, classified the forest soils of the higher elevations in the Great Smoky Mountains as Ramsey Soils (Soil Survey Staff, 1956). These soils are chiefly on steep slopes and vary considerably in depth and degree of distinction between profile layers. Soils derived from the Anakeesta Formation are Ramsey shaly silt loam, while those of the Thunderhead Sandstone are termed Ramsey stony fine sandy loam. The two types are both excessively drained and have low water-holding capacity (Soil Survey Staff, 1956).

Soil samples taken in the Mount Leconte area show that the dominant clay minerals are illite and vermiculite, with minor concentrations of kaolinite also present (Wolfe, 1967). Absent from the soil are 2:1 expanding lattice clays, which expand their lattices by absorbing water (Bogucki, 1970). Clay content is important in the consideration of potential slope instability because, as water content increases, clay materials lose their shear strength (Varnes, 1984). Organic matter content is variable and depends on the exposure, elevation, and vegetation (Ryan, 1989).

Vegetation

The study area is heavily forested, with the higher slopes covered by red spruce and Fraser fir and the lower slopes by a variety of hardwoods (King et al., 1968). The spruce and firs that dominate the boreal coniferous forest are present at elevations generally above 1676 m (5500 ft) (Whittaker, 1948). Rapidly-

reproducing hardwood species such as yellow birch predominate in revegetated debris slide tracks (Patric, 1976).

Many of the larger trees have very shallow root systems with a large tree height to root depth ratio. Because of this high ratio, tree throw is fairly common on steep slopes in the study area with trees being uprooted rather than sheared.

Climate and Weather

Due to the sharp changes in elevation and the high relief, the GSMNP contains a variety of microclimates. According to R. E. Shanks's application of the Thornthwaite climate system to the Great Smoky Mountains, the higher elevations possess a cool temperate rain forest climate, while a warm-temperate forest climate is found in the lower elevations (Shanks, 1954).

The Southern Appalachians have one of the highest annual rainfall totals east of the Cascade Mountains, with averages between 100-270 cm and maxima up to 380 cm (Neary and Swift, 1987). Precipitation maxima occur in late winter and late summer. While most winter precipitation is cyclonic in origin, summer rainfall is mainly from convective thunderstorm activity.

The difference in precipitation between the high and low elevations is considerable. The average precipitation in the Great Smoky Mountains is 163 cm/year, but the high elevations receive well over 203 cm annually (Whittaker, 1948). A water surplus exists throughout the year at all elevations above 1158 m (3800 ft), and only at 445 m (1460 ft) and below is precipitation less

than potential evapotranspiration at any month of the year (Shanks, 1954). Not only is there an increase in total rainfall with elevation, but there is a similar increase in rainfall intensity. Using data from six rain gauges during the period 1939-1968, Bogucki (1972) found a positive relationship between intense rains and elevation, with 194 of 250 intense rainstorms studied occurring above 1220 m (4000 ft).

Most of the intense rainfall occurs during the summer season. As defined by the Tennessee Valley Authority, intense rainfall is one or more inches of rain in one hour or three or more inches in twenty four hours (TVA, 1937). Such rainfall events are quite common, with 1273 intense storms recorded during the period 1951-1987 (Ryan and Clark, 1989). These intense rainstorms are the primary triggering agents for debris slides in the Appalachian Highlands (Bogucki, 1970; Scott, 1972).

Elevation differences affect temperature as well as rainfall. Temperature decreases an average of 1.2 degrees Celsius (2.2 degrees Fahrenheit) for each 305 m (1000 ft) increase in elevation in the Great Smoky Mountains (Shanks, 1954).

Anthropogenic Influence

There is little imprint of human impact in the study area. Although logging was widespread in the GSMNP in the early part of this century, most of the Mount Leconte area has never been logged (Bogucki, 1970). A single road, U.S. Highway 441, passes through the study area. This transmountain road closely parallels Walker

Camp Prong, and debris flows from Anakeesta Ridge have blocked it on several occasions, most recently in 1995. The only other marks of anthropogenic activity are the several trails that cross through the area. Like the roads, these trails have experienced extensive damage from debris slides in the past.

Previous Studies

The Mt. Leconte/Anakeesta Ridge area has been the subject of several debris slide studies. The first was by Bogucki (1970), who studied the erosional effects of a September, 1951 cloudburst in the area of Mount Leconte and Sugarland Mountain. Bogucki employed aerial photography in order to remotely identify debris slide tracks and made detailed planimetric sketches of 19 of these slides. He also assessed the importance of several slide inducing factors such as geology, hydrology, slope angle, and soils. Clark has studied the area extensively and reported on slides occurring in 1971, 1983, and 1984 (Clark, 1987; Clark et al., 1987). Clark's major area of focus has been Anakeesta Ridge, and his concept of assessing slope stability by limiting equilibrium analysis was later executed by Ryan (1989) in his studies. Feldkamp (1984) examined the revegetation of debris slide scars on Mount Leconte. The most recent, by Ryan (1989), involved research on the continuing expansion of slide scars and a slope stability analysis on Anakeesta Ridge.

Historical Slide Activity

Table 1 outlines a history of debris slide events in the study area. Landslide activity in the area has increased in frequency over the past several decades (Clark, 1987; Ryan, 1989). Compound scars have increased in extent and volume, and scars exhibit progressive backwasting toward the ridge crest (Ryan, 1989) (Figure 7).

Debris slides occurred most recently in response to rainfall associated with Hurricane Opal on 4-6 October 1995. In the early evening of 4 October, Opal made landfall in the Florida panhandle as a category 3 storm (National Climate Data Center, 1995). The hurricane was downgraded to a tropical storm by the early morning hours on the 5th. The storm track moved north-northeastward through Alabama and into Tennessee.

Table 1. Debris Slide History.

DATE	TYPE OF STORM	AREA NAME
10 Jul 1942	Thunderstorm	Newfound Gap
1 Sept 1951	Cloudburst	Mt. Leconte
15 Jun 1971	-	Mt. Leconte
March 1975- through 1983	Multiple storms	Anakeesta Ridge
Aug 3, 1978	Thunderstorm	Mt. Leconte
Mar/Sep 1985	Thunderstorm	Anakeesta Ridge
Jul 1984	Thunderstorm	Anakeesta Ridge
10 August 1984	Thunderstorm	Anakeesta Ridge
June 28, 1993	Cloudburst	Mt. Leconte
Oct 4-6 1995	Hurricane Opal	Mt. Leconte/Anakeesta

(Source: Clark, 1987)



Figure 7. Backwasting of Debris Slide Scars on Anakeesta Ridge.

Rainfall during the previous summer had been below normal, probably contributing to low antecedent soil moisture conditions. Bogucki (1970) states that, prior to the 1951 debris slide event, soils had been unusually dry as well. The storm system dropped 13 cm (5.13 in) of rain on Newfound Gap and 14.7 cm (5.8 in) at Mount Leconte (National Climatic Data Center, 1995). In the surrounding region, some of the heaviest rainfall totals were in the western North Carolina mountains with 26.5 cm (10.43 in) recorded at Mount Mitchell and 22.2 cm (8.74 in) at Grandfather Mountain. To the west in Knoxville, only 3.8 cm (1.53 in) of rain fell.

Wind velocities on the mountain peaks were quite high during the event; atop Mt. Leconte, wind velocities reached 113 kph (70 mph) (Knoxville News Sentinel, 1995). Peak wind gusts were only 82 kph (51 mph) at Knoxville, Tennessee (National Climatic Data Center, 1995).

The heavy rains and strong winds caused extensive damage in southeast Tennessee and the Great Smoky Mountains. Widespread windthrow occurred in the vicinity of Mt. Leconte and Anakeesta Ridge particularly. As an illustration of the destruction, 271 downed trees were found along an 8 km stretch of the Appalachian Trail (Daily Times, 11 Oct). Uprooted trees left holes in the ground as large as 3 m in diameter.

The storm triggered at least five debris slides in the area; the slide damage coupled with windthrow caused such extensive damage to trails that clean-up efforts continued more than six months after the event occurred. I identified five new slides

during field surveys and added these to the debris slide inventory for the area. Two of the slides crossed U.S. highway 441 early in the morning of October 5th, depositing debris that closed the road for a period of four days. The material had to be transported out of the park for disposal because the Anakeesta deposits generate highly acidic leachate which destroys aquatic biota in streams. The total costs for storm cleanup in the National Park were over \$1.4 million dollars (Daily Times, 1995).

Thus, debris sliding not only creates extensive damage but poses a definite hazard to humans in this portion of the Great Smoky Mountains. Because debris slides in the study area occurred as recently as 1995 and because debris slides recur, debris slide susceptibility research in this area is particularly important. The following chapter will discuss the methods used to determine primary slide-inducing factors and determine relative failure potential.

CHAPTER V

METHODS AND TOOLS

In this chapter, I present the data set and the methodology employed to determine relative susceptibility for debris sliding. The most important piece of the data set is the DEM of the study area, as many of the variables were derived from it. I discuss the process of determining the interrelationships between these variables and debris slide occurrence using GIS techniques. Lastly, I describe the two methods used to quantitatively assess varying levels of susceptibility across the study area.

Data Sources

The primary data source for computer analysis was a Digital Elevation Model (DEM) produced at the National Park Service Research Station at Twin Creeks, Gatlinburg, Tennessee by GSMNP employees. This DEM has a 30 meter resolution (cell size 30 m x 30 m), in the local Universal Transverse Mercator coordinate system, and is based on the 1927 North American Datum. The level of resolution, although coarse for site specific studies of landslide susceptibility, is appropriate for medium scale (1:50,000 to 1:25,000) hazard mapping (Rengers et al., 1992). In comparison, Gao (1993) utilized a 24 meter resolution DEM in his analysis of factors conducive to landsliding in a 28 square kilometer area in Virginia.

An Earth Resources Data Analysis Systems (ERDAS) coverage of the local geology in the Great Smoky Mountains National Park was also obtained from the research center at Twin Creeks. The resolution was coarser (90 m) than that of the DEM, but this was the only geologic coverage available. Karl Hermann, University of Tennessee faculty member, converted the coverage from ERDAS to ARC/INFO. I reduced the cell size to 30 meters to interface with the other data layers.

The final piece of the database was the debris slide locations. I mapped a total of 42 slides in the study area ranging in approximate area from 29,000 to 11,000 square meters. I identified previous debris slide/flow sites from published studies (Bogucki, 1970; Feldkamp, 1984; Ryan, 1989) and updated the inventory with the most recent activity. I used aerial photographs available at Twin Creeks to verify the location of landslide scars. Next, I field checked sites of accessible scars for accuracy. Although I attempted to verify the exact location of the slides using a Global Positioning System, the efforts proved fruitless as terrain and vegetation masking hindered satellite reception in the mountainous terrain.

I plotted the locations of the debris slides on USGS 7.5 minute quadrangles and then digitized the slides as polygons. Next, I converted the polygon coverage from vector to raster format at a 30 meter resolution to match the DEM resolution. Although several slide tracks are slightly less than 30 meters in width, the resolution is adequate to depict their general locations. While

mass movements can be depicted as points (Wadge et al., 1993), when the actual dimensions of the slide are considered important, their representation should conform as closely as possible to their true shape.

Variable Selection

The central problem in this study was to determine those conditions which make a slope in the study area most susceptible to failure. Because there are many parameters considered important to debris sliding, a crucial step in analysis is to select sound, relevant factors. According to Aniya, it is critically important to include parameters that have played a significant role in landsliding and that can be measured in sufficient detail for their areal distribution to be mapped (Aniya, 1985). Variables used in the analysis were limited to those which could be derived from the available data set just described.

The independent variables chosen for the analysis include slope angle, slope aspect, slope form (plan and profile), geology, distance from ridge crest, and precipitation; the dependent variable is presence/absence of landslides. The following is a description of these variables and how they affect slope stability.

Slope Angle

Slope or slope steepness has always been an important and widely used topographic attribute in studies of slope stability (Moore et al., 1991). Slope angle is the first derivative of

elevation and represents the ratio of the rise of the slope to the run (Franklin, 1987). The magnitude of the downslope component of gravity increases directly with slope gradient.

Numerous studies of slope failures have shown that slope steepness has a strong effect on failure occurrence. Although the competency of the bedrock may offset the effects of steep slopes, landslides generally occur above a minimum slope angle (Jibson and Keefer, 1989). Pariseau and Voight (1979) found that slides in the Appalachians occur where slope angles range between 17 and 44 degrees (Pariseau and Voight, 1979).

While the above cited studies found that slides tend to occur at certain slope angles, the question arises concerning whether or not the hillslope angles on which the slides initiated were created by the landsliding process itself. According to Carson and Kirkby (1972), little attention is paid to the role mass movements play in shaping the sides of hills and valleys. However, more recent studies have shown that, depending on the nature of the local structure and its discontinuities (cleavage, bedding planes, joints), landslide events may play a significant role in forming side slopes and their associated angles (Ryan, 1989; Moore, 1997).

Slope Aspect

Slope aspect is the directional component of slope. It is commonly specified as the direction on the compass, usually in categories (Franklin, 1987). Slope aspects are categorized in order to identify general trends in certain phenomena occurring on

different slope azimuths. Aspects can also be portrayed as scalar values by computing the degree difference from a certain heading, such as south (180 degrees).

Aspect has a strong influence on local climate. In mountainous regions, differences in microclimate are largely driven by solar illumination (Band and Moore, 1995). Slopes that receive greater amounts of solar radiation have higher temperatures and greater evaporative opportunity (Moore et al., 1991). Therefore, the direction that a slope faces will have a considerable effect on the amount of moisture retained by the hillslope (Carson and Kirkby, 1972).

Because of the differences in direct solar radiation reception, north facing slopes in the northern hemisphere have a high moisture content relative to south facing slopes. Higher and more prolonged antecedent moisture conditions make shady slopes more susceptible to failure-triggering events (Crozier, 1986). Gryta and Bartholomew (1987) determined that in central Virginia, slopes in the northern quadrant (330-090 degrees) were the most likely to fail.

However, although north facing slopes are wetter in general, antecedent moisture conditions do not always dictate which slope aspect will be the most failure prone. The dip of the rock strata is also very important. Slopes on which the strata dip in the same direction that the slope faces are known as dip slopes, and the opposite slopes are termed scarp slopes. Varnes (1984) found that where the land surface slopes at more than 15 percent, within 45

degrees of the direction in which the strata dip (a dip slope), the area is susceptible to failure. Gupta and Joshi (1990) concluded that landslides in the Himalayas are more frequent in the direction of the dip. Studies by Bogucki (1970) of debris slides in the Mt. Leconte area showed that most slides occur on south facing slopes, suggesting that the southerly dip of the beds in the area influences failure susceptibility.

Slope Form

Slope morphology is one the most important influences on landsliding because it affects the movement of surficial materials, surficial runoff, and soil water (Aniya, 1985). Local surface curvature, or convexity, is defined as the rate of change of slope or the second derivative of elevation (Franklin, 1987). Slope form can be described as concave, convex, or rectilinear in both profile (downslope) and plan form (cross slope). A slope is convex when the rate of elevation change increases downslope between points that are close together; in concave forms, the rate of elevation change decreases between points when moving downslope (Franklin, 1987). On rectilinear or straight slopes, the slope angle is approximately constant.

Profile curvature is the curvature of a surface in the direction of slope and is an important determinant of erosion and deposition processes at the hillslope scale (Moore, et al., 1991). Where the curvature is convex, the profile is positive, slope is increasing, and erosion occurs because of the increased ability to

transport particles as water flow accelerates (Moore, et al., 1991). Where the curvature is concave, the profile is negative, slope is decreasing, and deposition tends to occur (Chorley et al., 1984; ESRI, 1994). Concave slopes give some basal support to potential slide masses. Convex slopes, on the other hand, do not provide support at their bases (Carson and Kirkby, 1972).

The characteristic slope profile of humid temperate areas consists of a convex upper part and a lower concave slope with a short straight segment often present in between (Carson and Kirkby, 1972). While the upper convexity is normally attributed to a combination of weathering and creep, the concave base may be, essentially, a depositional feature. Hack and Goodlett (1960) attributed basal concavity in the Central Appalachians to the tendency of streams to adjust their slopes to the volume of water they contain in order to equalize the work of sediment transport. The straight slope section tends to be more prevalent in areas of high relief, probably because straight segments are quickly obliterated in the slope profile in lowland areas (Carson and Kirkby, 1972).

Planform curvature is the shape of a surface perpendicular to the direction of slope (ESRI, 1994). The plan form is especially important as it dictates the area of converging or diverging water flow (Aniya, 1985). Where the curvature is concave, flow converges (runoff is concentrated), whereas flow diverges where curvature is convex. Convex surfaces indicate ridges, while concave surfaces indicate valleys. Concave depressions have been termed "hollows"

and the intervening area between two adjacent hollows is known as the "nose" because of the convex outward topography (McKean et al., 1991).

Hollows normally have a higher soil water content than noses, even without a water table, perched water, or impermeable layer near the surface (Zaslavsky and Sinai, 1981). The greater thickness of colluvium in hollows and the topographically-induced surface and groundwater concentrations there make hollows a primary source of debris flows (Reneau and Dietrich, 1987; McKean et al., 1991). In studies by Reneau and Dietrich (1987) in Marin County, California, hollows were the most important landform source of landslides, accounting for 62% of the scars by number.

Lithology

Lithology includes the composition, fabric, texture, and other attributes that influence the physical or chemical behavior of rocks and soils (Varnes, 1984). Lithology is one of the most important factors influencing the factor of safety (FS) (Torbett and Ryan, 1986). Slope stability conditions vary significantly with the type of material involved, and this relationship has been shown in numerous studies (Schneider, 1973; Newman et al., 1978; Gryta and Bartholomew, 1987; Jacobson et al., 1987b; Carrara et al., 1991). These variations exist because of differences in shear strength, permeability, and susceptibility to chemical and physical weathering.

Distance from Ridge Crest

Debris slide susceptibility has also been related to the distance downslope from the ridge crest (Reneau and Dietrich, 1987; Aniya, 1985). This variable is indicative of water catchment area because, as distance increases, the amount of water accumulating and flowing downslope increases. There is a strong tendency for soils to be thin on narrow ridges and relatively thick on the lower slopes; with increasing soil thickness, slopes become more unstable (Dietrich et al., 1995).

However, the relationship between distance from ridge crest and debris slide occurrence is not always clear. Reneau and Dietrich (1987) found that slide headscarps were located as close as 10 m below ridge crests. This suggests that sufficient water for failure may, in some cases, be provided by rainfall directly onto the site, with little contribution of subsurface runoff from upslope. However, this may also suggest that scarheads have gradually backwasted toward the ridge crests, as is the case on Anakeesta Ridge (Ryan, 1989).

Precipitation

Next to gravity, water is the most important factor in slope instability (Varnes, 1984). Rainfall increases the pore water pressure in the subsurface, which reduces shearing resistance (Pariseau, 1979). Clark, Ryan, and Drumm (1987) found that the primary slide triggering mechanism on Anakeesta Ridge is an increase in pore pressure during high precipitation events. When

water replaces air in soil interstices, cohesion decreases. Water can be absorbed by the regolith, thereby increasing its weight and adding to the downslope component of stress. The rate of weathering is influenced by the amount of moisture available (Bell, 1983).

In many cases, elevation is used as an indirect means of accounting for spatial variations in precipitation and/or temperature (Moore et al., 1991). Weather and climate conditions vary greatly at different elevations, and this is reflected in differences in soil and vegetation (Aniya, 1985). As precipitation amounts tend to increase with increased elevation, the likelihood of slope failure should likewise increase.

In this study, I computed a rough estimate of annual precipitation through the elevation profile based on data obtained in a precipitation-altitude study by Smallshaw (1953) in the GSMNP. In Smallshaw's study, precipitation data were collected from eight precipitation gauges during the years 1946-1950. The location of the gauges, which range in elevation from 445 m to 1920 m (1460 to 6300 ft), is shown in Figure 8. The gauges were established along U.S. Highway 441, which passes through the center of the Mt. Leconte - Newfound Gap study area. Therefore, the data gathered were well-located to represent the general precipitation pattern in this portion of the GSMNP. Based on the 5-year mean precipitation values for the eight stations, I established a regression relationship to estimate precipitation from elevation.

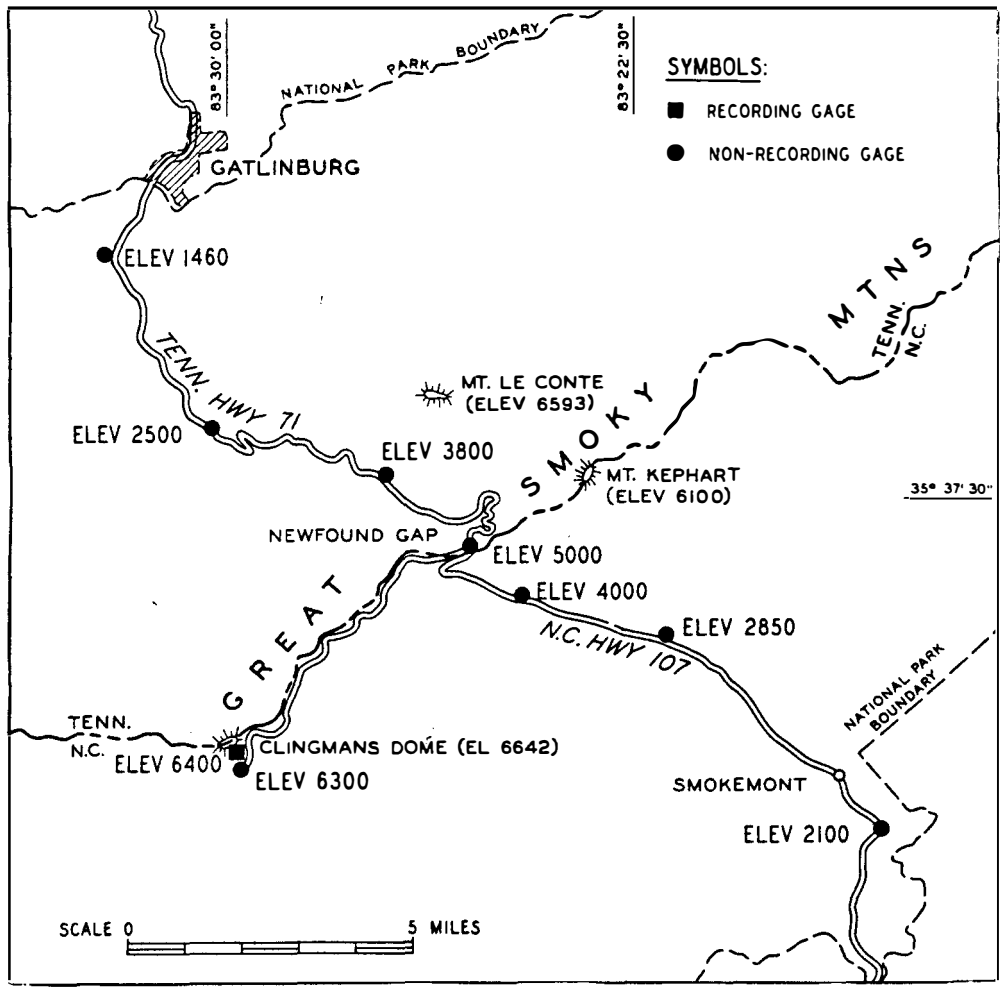


Figure 8. Map of Precipitation Gauge Locations.
 (Source: Smallshaw, 1953)

The equation relating the two variables is:

$$\text{Precipitation} = 32.155 + .0184 (\text{Elevation}) + .00000143 (\text{Elevation})^2$$

where Precipitation is in inches/yr and Elevation is in feet.

Although the R squared for this regression equation is .96 and is significant at the .02 level, this relationship is only a raw estimate since it is based on a sample of eight points. The equation does not take into account the effects of aspect or relief on precipitation totals. Moreover, the annual precipitation values do not reflect the number of intense rainstorms occurring at altitude, which serve as triggering agents of debris slides. However, Bogucki (1972) found that intense rainfall, like total precipitation, is directly related to elevation in the GSMNP. Despite the shortcomings of the data set, the data were considered representative enough to use in the analysis, realizing, of course, that the precipitation values are by no means exact.

Existing Slides

According to Varnes (1984), the most important geomorphologic characteristic for determining landslide susceptibility is the presence or absence of former landslides. Because the most common landslide mechanism is the reactivation of old slides, evidence of past instability is frequently the best guide to future behavior in the area (Wadge, 1993; Varnes, 1984). Slope failures may initiate further slope movement upslope (retrogressive) or downslope

(progressive) by steepening slopes at their heads and adding surcharges below (Jones, 1992). In this study, the location of debris slide scars will be used to determine the combination of factors that are most conducive to slope failure.

Variables Not Considered

Several factors were not included in the study due to lack of sufficient data or personal judgment on the relative importance of these factors in the study area. Soil properties were not incorporated owing to lack of data, but previous studies indicate that soil type is probably not a determining factor. Wind also seems to be a significant variable as shown by Bogucki (1970) and Ryan (1989). Windthrow creates a lever effect on the surface which pries the soil and produces hollows where water may drain into the subsurface. Mapping the spatial extent of tree throw in the study area would have been too time intensive, and the spatial pattern of tree throw probably contains a large chaotic component. Because the entire study area is forested, vegetative cover was not included as a separate variable. In general, tree roots contribute to slope stability by increasing cohesion and drawing up moisture through evapotranspiration. The role of trails in debris slide susceptibility was not examined, although they appear to have some influence on debris slide location (Bogucki, 1970).

Hardware/Software Tools

I conducted the computer analysis with the ARC/INFO GRID software package on a Sun workstation. A wide range of sophisticated applications is available to compute topographic attributes in ARC/INFO GRID, with little requirement to create new algorithms. GRID commands were used to compute slope angle, slope aspect, elevation, ridge distance, and slope form (profile/plan form) from the Digital Elevation Model. Procedures are outlined in Appendix A.

Debris slide polygons were digitized using ARC/INFO's ARC Digitizing System (ADS) software. ADS is a system used to digitize and perform edits on line, area, and point features (ESRI, 1993). I transformed the debris slide polygon coverage from vector to raster format in GRID on the Sun workstation. The debris slides are shown in Figure 9 with a background of the topography to provide spatial reference.

Analysis Techniques

Two types of analysis were used to develop a debris slide susceptibility map and evaluate the relative importance of the independent variables: (1) failure rate analysis and (2) logistic regression.

Failure Rate Analysis

Failure rate analysis is founded on data normalization procedures in which the percentages of landslide-affected area

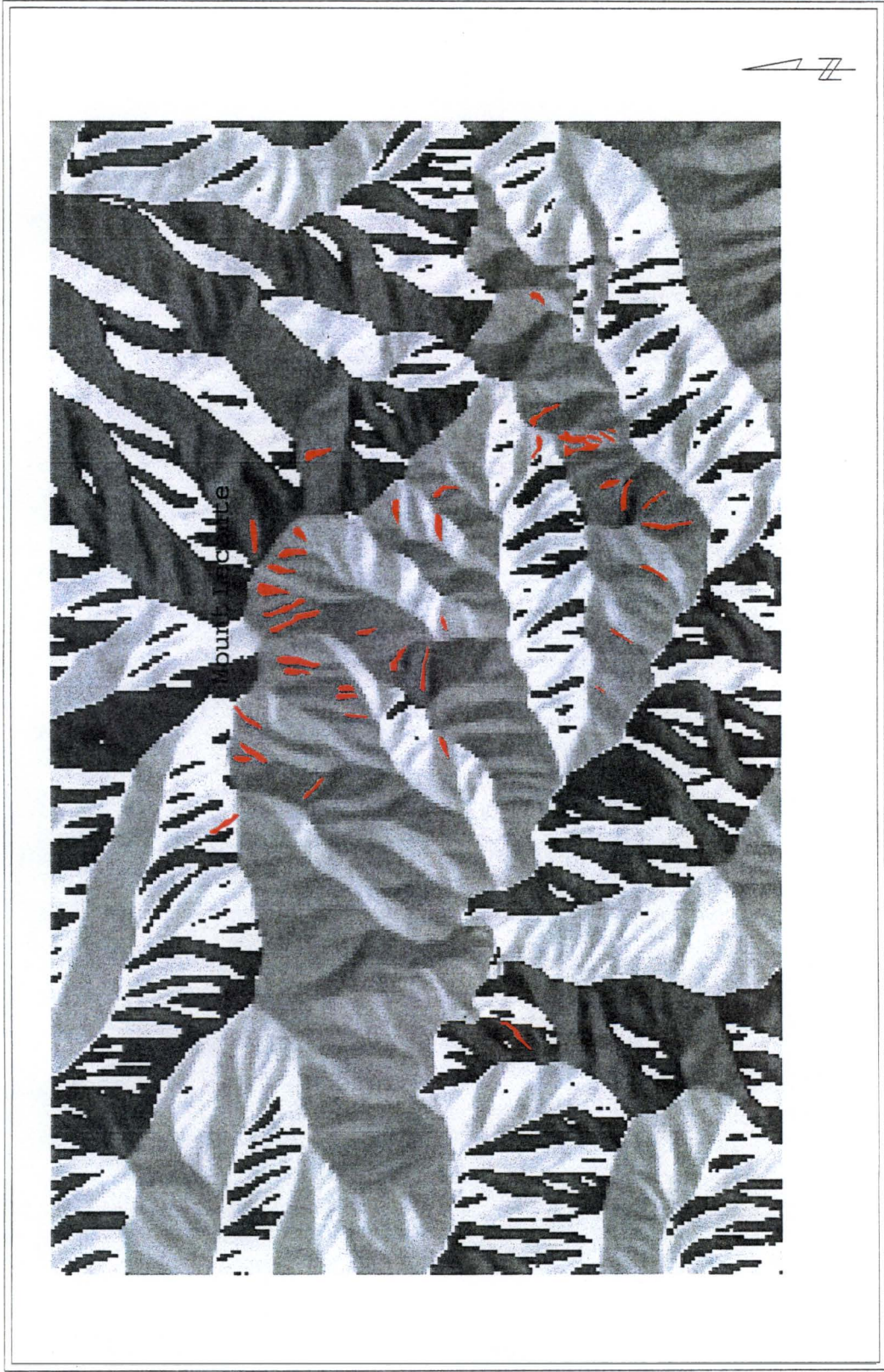


Figure 9. Map of Debris Slide Locations. (shown in red)

associated with a particular factor are divided by the areal extent of that factor (Dikau, 1990). "Affected" cells are those which are contained completely in a debris slide scar; in other words, they are one of the cells which makes up an individual scar. The failure rate (FR) reflects the importance of this attribute to the occurrence of landslides relative to the entire study area (Dikau, 1990). Failure rate analysis was employed by both Aniya (1985) and Dikau (1990) in their studies of landslide susceptibility.

The first step in failure rate analysis is to subdivide the variables into discrete classes. The variables and their respective classes for the Mount Leconte study area are shown in Table 2. The resultant grids for each variable are shown in Figures 10-16. Next, the number of grid cells that belong to each class is divided by the total number of grid cells in the entire grid matrix; the result is the relative frequency (RF) of this class in the entire study area. A general equation for RF is as follows:

$$RF = \frac{\text{Total cells in class "m"}}{\text{Total number of grid cells}}$$

Next, the number of cells "affected" by debris slides within each class is divided by the total number of cells affected by debris slides; the result is the relative frequency (RF) of this class in debris slide areas. The number of affected cells in each class is computed by overlaying the debris slide layer with the respective attribute layer associated with that class.

Table 2. Failure Rate Variables and Classes.

Class	1	2	3	4	5	6	7	8	9	10	11
Variables											
Slope (degrees)	0-5	5-10	10-15	15-20	20-25	25-30	30-35	35-40	40-45	45-50	50+
Aspect	N	NE	E	SE	S	SW	W	NW			
Slope Plan Form	straight	concave	convex								
5 3 Slope Profile Form	straight	concave	convex								
Lithology	Thunderhead Sandstone	Elkmont Sandstone	Anakeesta Formation								
Distance to Ridgecrest (m)	0-45	45-90	90-135	135-180	180-225	225+					
Precip (cm)	175-180	180-185	185-190	190-195	195-200	200-205	205-210	210-215	215-220	220-225	225-230

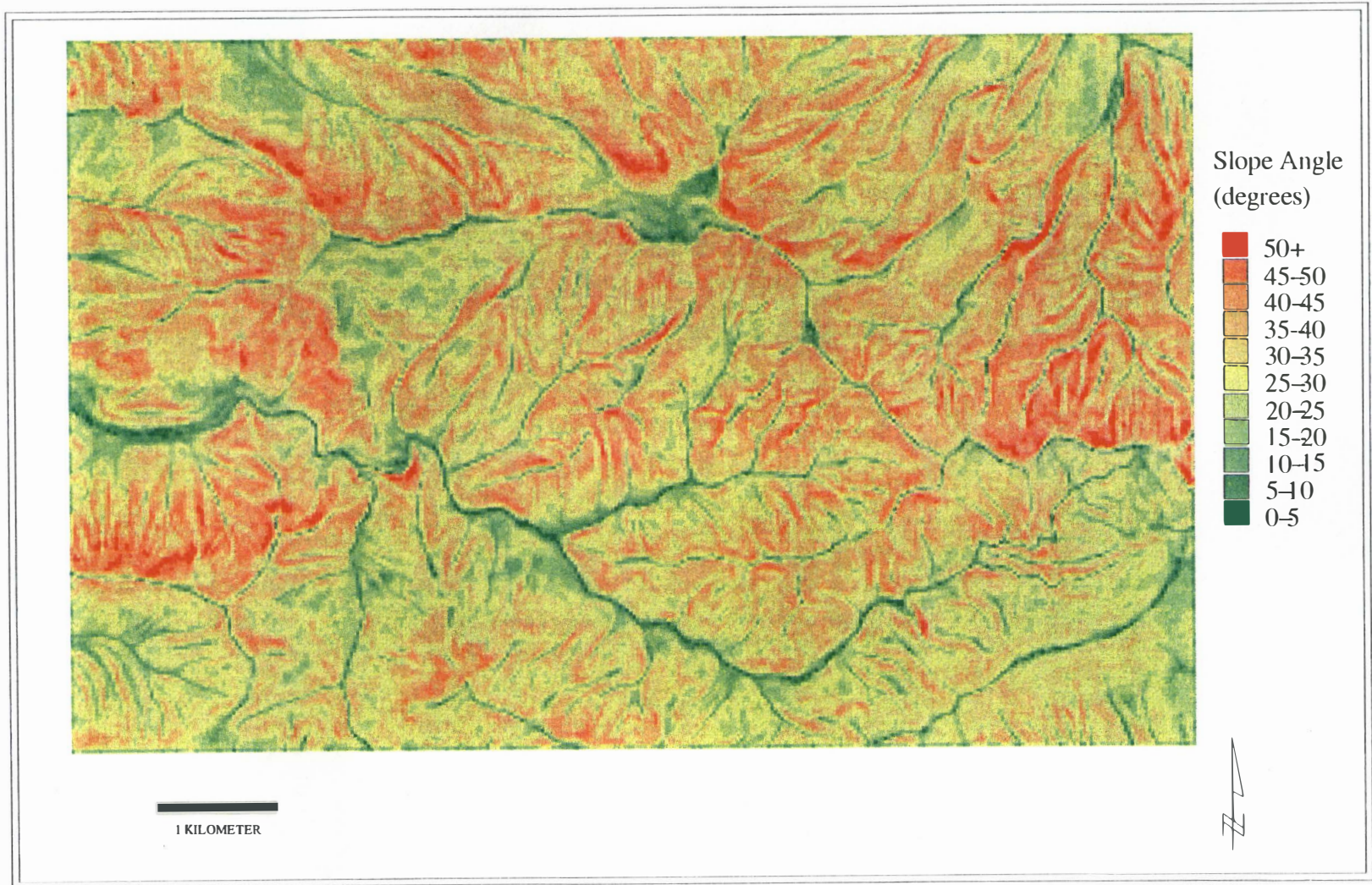


Figure 10 . Map of Slope Angle Classes .



Figure 11 . Map of Slope Aspect Classes .

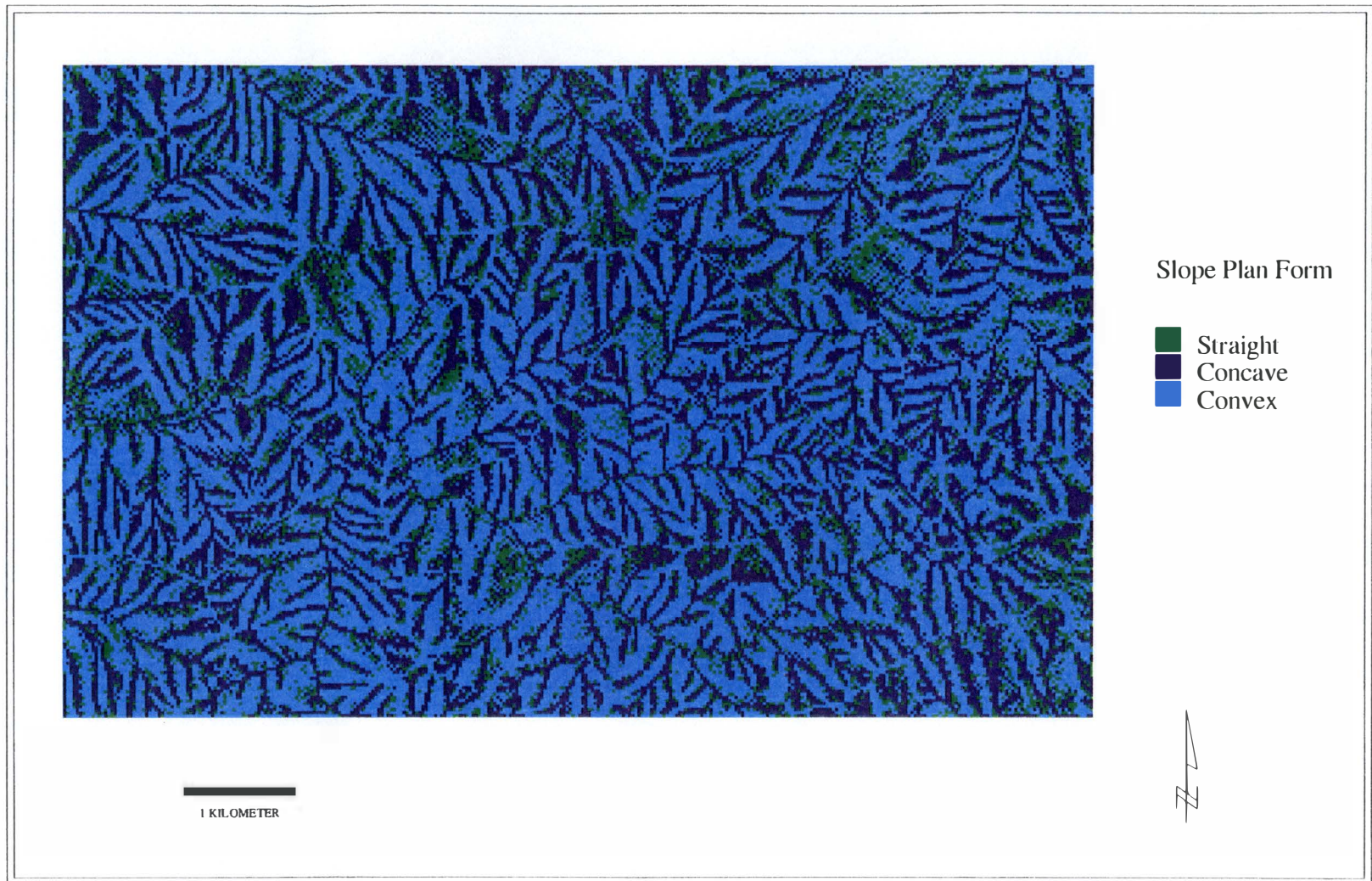


Figure 12 . Map of Slope Plan Form Classes .

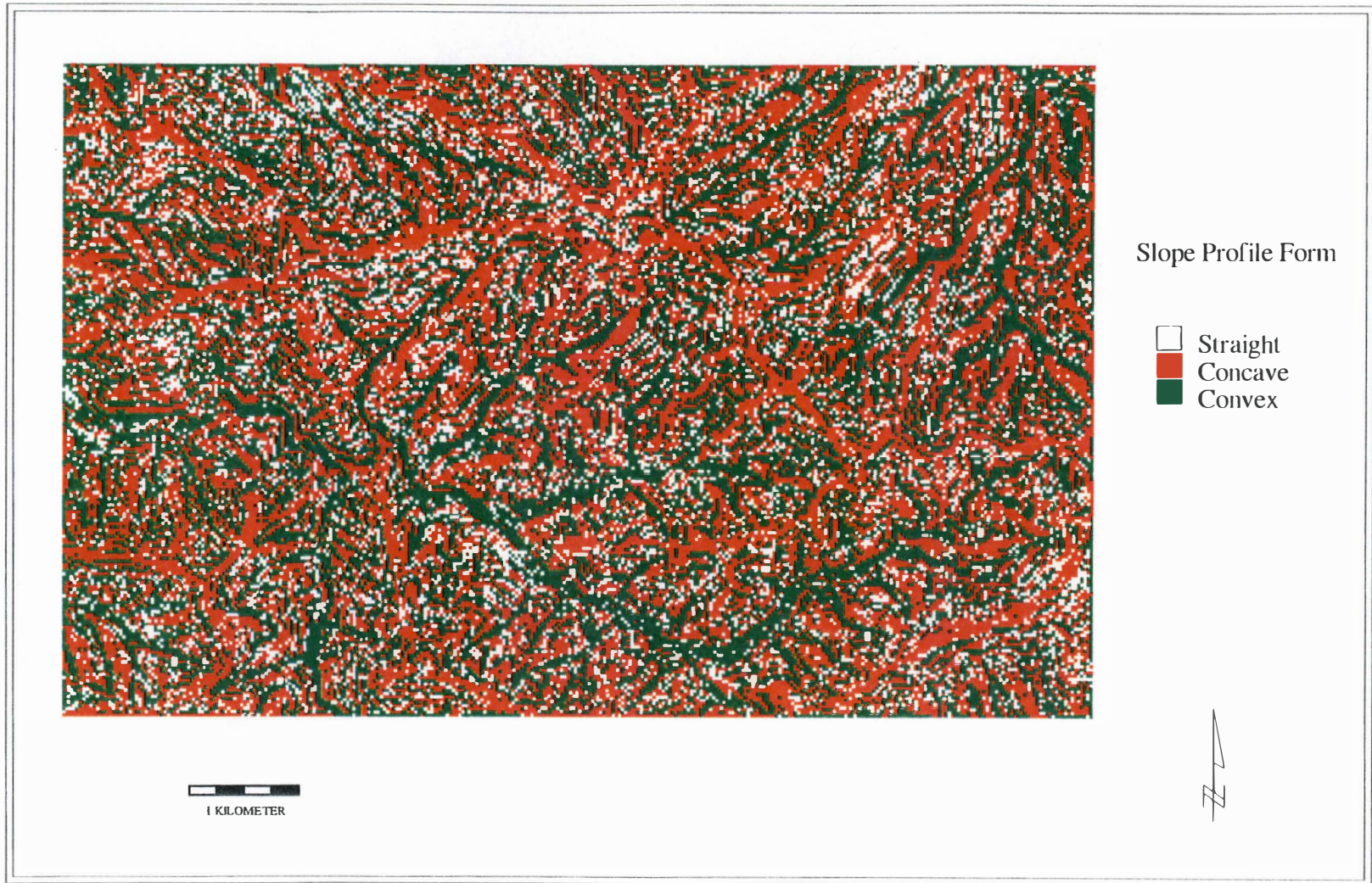


Figure 13 . Map of Slope Profile Form Classes .



Figure 14 . Geologic Formations in the Study Area . (Source : Data from GSMNP)

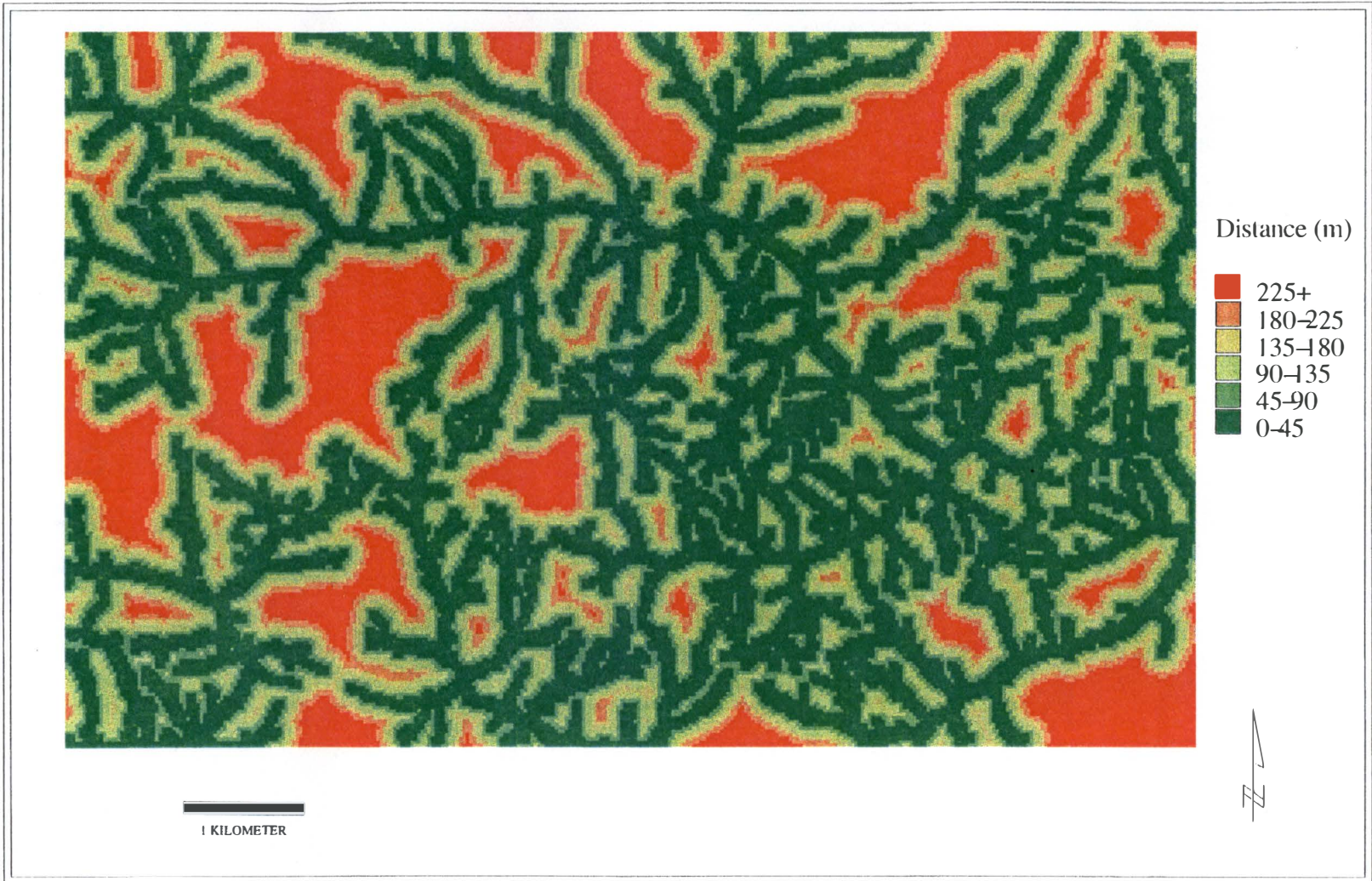


Figure 15 . Map of Distance from Ridge Crest Classes .

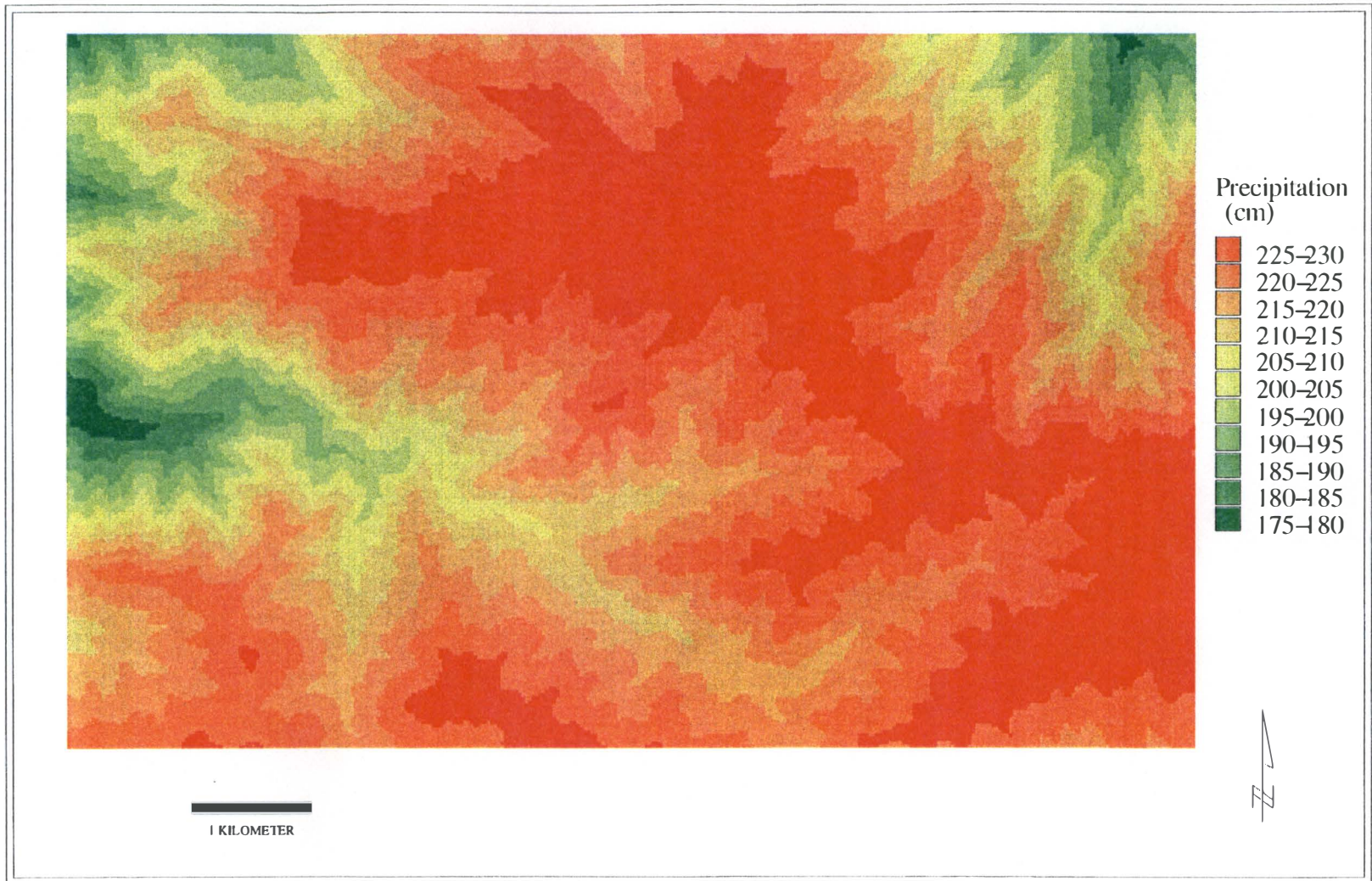


Figure 16. Map of Annual Precipitation as Extrapolated from Data of Smallshaw (1953) .

The failure rate (FR) is calculated by dividing the RF for debris slide areas by the RF for the entire study area. This is the formula for computing failure rate:

$$FR = \frac{\text{RF for landslide areas}}{\text{RF for the entire study area}}$$

A value greater than 1 signifies that the attribute contributes to landsliding, while a failure rate less than 1 shows that the attribute inhibits landsliding (Aniya, 1985). Although utilizing FR = 1 as a discriminating point between slide producing and slide inhibiting factors is a broad generalization, the failure rate provides a useful means of weighting factors for use in an evaluative model to construct a debris slide susceptibility map.

The debris slide susceptibility map based on failure rate values was produced using the following method. Once the failure rate for each class was determined, this failure rate value was substituted for the original attribute value for the respective class. The next requirement was to produce a grid which integrated the failure rate values from each of the six data layers.

This was accomplished by first adding the failure rate values for all six data layers together (a computer arithmetic operation), resulting in a composite grid whose cell values represent the aggregated effects of all variables. Each variable is weighted by the magnitude of the failure rate value. I then chose four susceptibility categories based on the relative probability of

future slide activity: very low, low, medium, and high, representing an ordinal scaling of susceptibility. In order to delineate four susceptibility categories, I set the maximum value of all composite cell values to 100 percent and selected categories based on a percentage of the maximum value. The following probability categories were established: very low (0-25 %), low (25-50%), medium (50-75%), and high (75-100%).

This type of analysis is well suited to Geographic Information Systems because areal coverage of factors is easily computed by looking at the number of cells affected. Although this model is an oversimplification of slope stability phenomena, this method can provide an adequate assessment over a large area for which the resolution of the data is not particularly high (Dikau, 1990).

Logistic Regression

In logistic regression, the known values of the dependent variable are represented by the presence or absence of the phenomenon at the sample locations (ESRI, 1994). Based on the attributes contained at a particular location, logistic regression predicts the relative probability of the phenomenon occurring at each location (ESRI, 1994). In this study, the phenomenon being predicted is the presence or absence of debris slides, which is a binary event. Therefore, the observed value of the dependent variable will be 1 (landslide is present) or 0 (no landslide).

Recent works employ logistic regression as a statistical tool in landslide mapping. Bernknopf et al. (1988) applied logistic

regression utilizing the SAS statistical procedure, LOGIST, to develop several models which calculated the unique landslide probability for each cell in a grid. A logit regression model was also used to produce a debris flow probability map of San Mateo County, California (McKean et al., 1991).

Logistic regression has several advantages over other statistical techniques. First, there are far fewer assumptions required than in linear discriminant models so that logistic regression is often preferred over discriminant analysis (Harrell, 1983). Secondly, this technique supports a variety of data types. Logistic regression supports nominal dependent variables and independent variables of interval, ratio, and nominal type. It is therefore well suited to the available data set (Wadge et al., 1993). In the present study, the dependent variable is the presence/absence of debris slides, and the independent variables are similar to those used in failure rate analysis, except as modified below.

The same basic variables that were used in the failure rate analysis were examined using logistic regression. However, unlike failure rate analysis, logistic regression can accommodate scalar values for the independent variables. This capability allows information, which would be lost in categorization, to be retained. Therefore, scalar values were used when possible, and certain variables were modified in order to make their values statistically meaningful.

The cell values for slope angle, distance from ridge crest, and precipitation did not require modification and were computed using the procedures outlined in Appendix A. Slope form was represented by two variables, profile and plan forms. Lithology was changed to reflect the presence or absence of the Anakeesta Formation in the cell, with Anakeesta cells receiving a value of 1, and all others, a value of 0. This type of binary variable is known as a "dummy" variable.

Likewise, the value for the dependent variable became 1 or 0, representing the presence or absence of a debris slide cell, respectively. In logistic regression, the number of values of the dependent variable representing the presence of a phenomenon (1) must approximately equal the number representing absence of the phenomenon (0). Hence, I made a random sampling of cells containing no debris slides which equaled the number of debris slide cells (428). This sampling was accomplished using a random cell selection process accommodated by GRID commands.

Because aspect values are circular, cell values for aspect had to be transformed into a distance from a particular azimuth. First, a two vector variable was computed representing degree distance from south (180 degrees) and distance from east (90 degrees). An additional vector representing degree distance from direction of dip (southeast) was also computed. The procedures for computing these vectors are outlined in Appendix B.

From the data sample, an ASCII file containing the values of the dependent and independent variables for each cell was created.

The data set was subjected to statistical analysis using the SPSS software package. Mr. Bob Muenchen of the University of Tennessee Statistical Consulting Center entered all values and ran the program, and I told him which variables to input and which procedures to execute. The resulting logistic regression function reflects the relationship between the attributes contained in a particular cell and the presence or absence of a debris slide.

The general form of the logistic regression function in SPSS is:

$$p = \frac{1}{1 + e^{-z}}$$

where Z is the linear combination:

$$Z = B_0 + B_1X_1 + B_2X_2 + \dots + B_iX_i$$

where B_i = coefficients of regression
 X_i = independent variables

(From Norusis, 1992).

The logistic regression function was used to create a map showing the probability of debris slide occurrence. Because the product of the logistic function is a probability (0-100%) for each cell, the grid was readily separated into four probability categories which were very low (>25%), low (25-50%), medium (50-75%), and high (75-100%). These probability categories were selected to coincide with those used in the failure rate analysis map for purposes of comparison.

CHAPTER VI

RESULTS AND DISCUSSION

In this chapter, I present and discuss the results of both the failure rate and logistic regression analysis. The maps produced by the two techniques vary considerably; I explore their differences and their particular merits. Both maps have their limitations, and I discuss these limits as well as some of the uncertainties of the analysis.

Results indicate that slope angles in the 35-40 degree range are the most susceptible to failure and that south facing slopes are most failure prone. Slopes that are concave in cross section are more susceptible than other slope forms. The rock type with the highest degree of susceptibility is the Anakeesta Formation. Ridge distances that are slightly below the ridge crest have the highest incidences of failure. Susceptibility tends to increase with the amount of precipitation received on slopes. The failure rate map places 75% of the existing slides in the medium-high probability range, while the map produced by logistic regression has 85% of slide areas in the medium-high range.

Failure Rate Analysis

Table 3 summarizes the results of the failure rate analysis by ranking the attribute classes by failure rate. From this table, the most significant descriptors of the landslides in the study

Table 3. Ranking of Attribute Classes by Failure Rate.

RANK	ATTRIBUTE (FACTOR)	CLASS	FAILURE RATE
1	Aspect	South	2.8
2	Aspect	Southeast	2.4
3	Precipitation	225-230 cm	2.3
4	Slope Angle	35-40 degrees	2.1
5.5	Lithology	Anakeesta	2.0
5.5	Aspect	Southwest	2.0
7.5	Slope Plan Form	Concave	1.9
7.5	Dist Ridge Crest	45-90 m	1.9
9	Slope Angle	40-45 degrees	1.8
10	Dist Ridge Crest	90-135 m	1.7
11.5	Slope Profile Form	Convex	1.3
11.5	Precipitation	220-225 cm	1.3
13	Slope Angle	45-50	1.2
14.5	Dist Ridge Crest	135-180 m	1.0
14.5	Slope Angle	30-35 degrees	1.0
14.5	Slope Profile Form	Straight	1.0

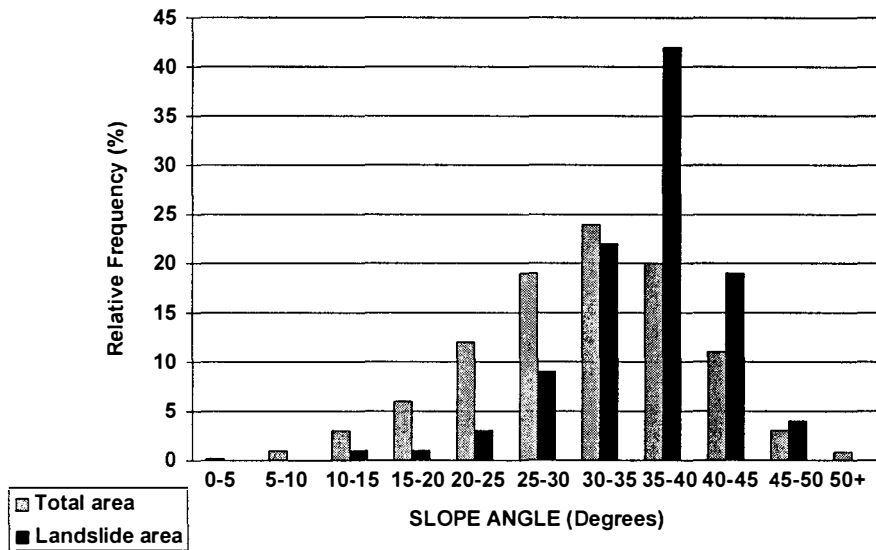
area appear to be south/southeast aspects, high precipitation (225-230 cm), and slope angle (35-40 degrees). Each attribute and its contribution to landslide susceptibility is discussed below.

Slope Angle

Figure 17 shows the relative frequency and failure rates of slope angles in each attribute class. Almost 60% of the study area contains slopes greater than 30 degrees. Slope angles tend to group around the 30-35 degree range, and this is characteristic of the tendency of slopes to group closely about a mean value (Strahler, 1950). Although slope angles ranging between 30 and 35 degrees dominate within the area, the range with the highest frequency of failures (35-40 degree) had the second largest areal extent. Slopes in the 35-40 degree range also had the highest failure rate (2.1). This generally agrees with Bogucki's findings of an average gradient of 40 degrees for slides in the Mount Leconte area (Bogucki, 1970).

The failure rate for all slopes of less than 30 degrees was less than unity, indicating that these slopes are not generally prone to sliding. All slopes between 35 and 50 degrees had failure rates greater than 1, but no failures occurred on slopes above 50 degrees. The results of this study are consistent with those of other studies in the Appalachians in which average slope angles on slides were found to be 35 degrees (Schneider, 1973), 37 degrees (Koch, 1974), and 33 degrees (Pomeroy, 1984).

(a) SLOPE ANGLE : Relative Frequency



(b) SLOPE ANGLE : Failure Rate

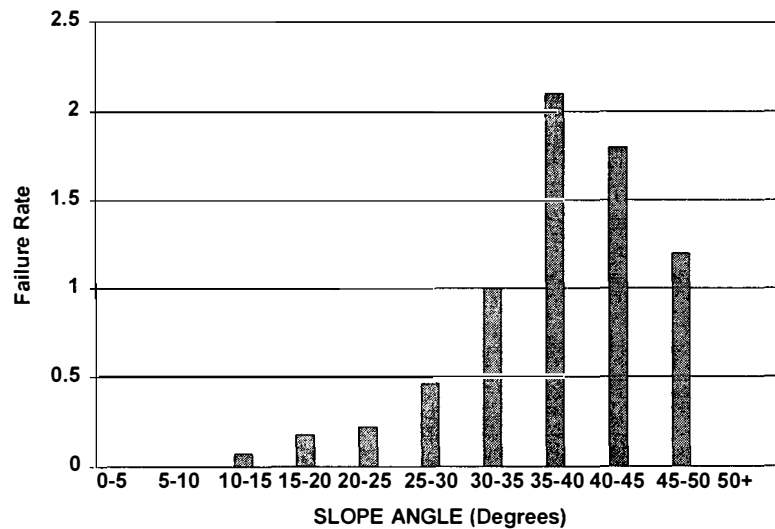


Figure 17. Relative Frequency and Failure Rate for Slope Angle.

The results indicate a definitive slope angle range within which slopes fail which is 30-50 degrees. Below the minimum, gravitational forces are not adequate to initiate slippage. Above the maximum, a decrease in water percolation or an increase in cohesion may cause the slope to be less failure prone. Dietrich et al. (1994) state that very steep slopes may be less susceptible than lower gradient slopes because destabilizing pore pressures build up with less rainfall on lower gradient hillslopes. Extremely steep slopes have characteristically thin and rocky soils due to rainwash and other erosion processes (Chorley et al., 1984). This is true in the Great Smoky Mountains where steep slopes are covered with a relatively thin residuum (Ryan, 1989).

Although this study and others cited above have established average slope angles at which slides tend to occur, they do not attempt to address the role that these mass movements play in shaping hillslopes. While sliding may occur on slopes whose shape has been determined by geomorphic processes other than debris slides, in some instances, the failure itself may have transformed the hillslope gradient. An excellent example of this phenomenon appears to be evident on Anakeesta Ridge. According to Ryan (1989) and Moore (1997), the debris slides on Anakeesta Ridge seem to have initiated as wedge failures and progressively developed into true debris slides. Wedge failure, a type of mass movement defined by geometry, occurs where a "wedge" is formed by the intersection of two planar discontinuities such as bedding planes, joints, and/or cleavages (Baird, 1990). Planar discontinuities are abundant in

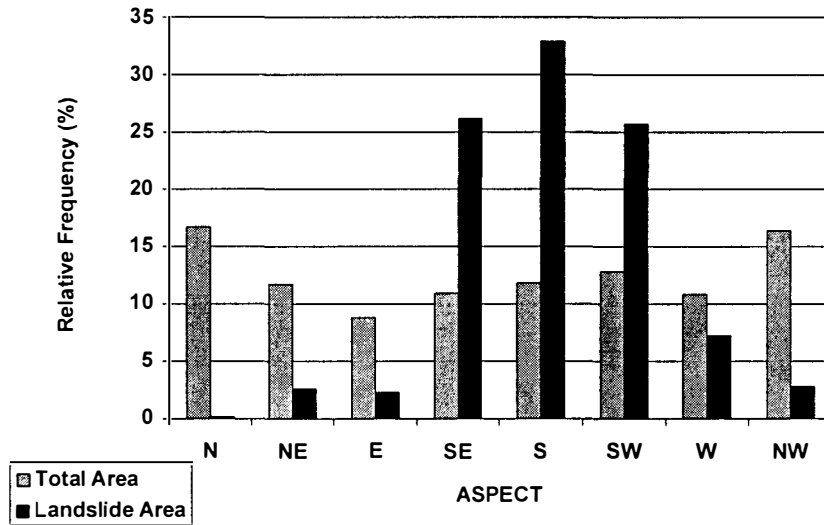
the Anakeesta Formation due to intense folding and faulting. When the wedge is displaced downslope, the result is a v-shaped ravine with characteristically steep sides (Moore, 1997). In the study area, bedding planes dip at angles ranging between 26 and 55 degrees (Bogucki, 1970). When the release surface for the failure is along these bedding planes on dip slopes, the exposed bedding coincidentally controls the resulting hillslope angle. Thus, the hillslope gradient may, in some instances, be largely dictated by pre-established planes of failure along discontinuities.

Slope Aspect

Figure 18 shows the relative frequency and failure rates of slope aspects in each class. North facing aspects (338-23 degrees) predominate, but most failures (33%) occur on slopes with a southerly aspect (158-203 degrees). Eighty five percent of the slides occur on south, southeast or southwest facing slopes. South facing aspects ranked third among all attribute classes in failure rate (2.8). Less than 3% of the slides occurred on either north or northeast facing aspects.

Although north facing slopes generally have a higher moisture content, southerly aspects are more failure prone in this area due to the regional dip to the southeast. Therefore, the aspect variable in this study appears to represent dip, a geologic variable, rather than the climatic variables often associated with aspect. On dip slopes, slip is facilitated along bedding planes. Moreover, greater moisture may be supplied to the surficial mantle

(a) ASPECT : Relative Frequency



(b) ASPECT : Failure Rate

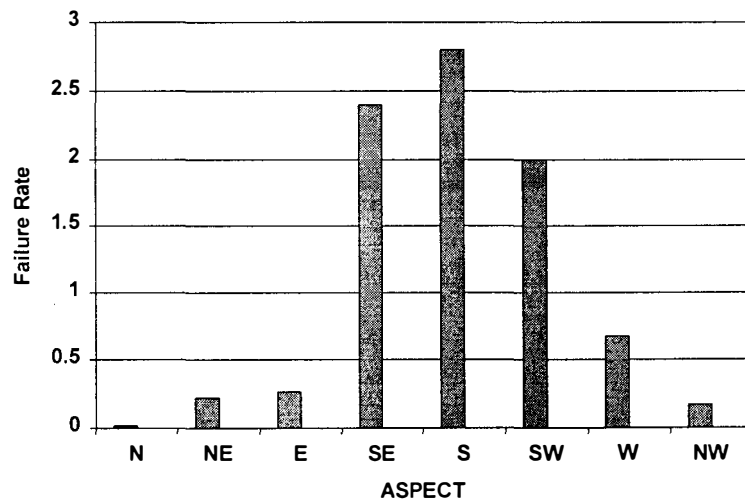


Figure 18. Relative Frequency and Failure Rate for Slope Aspect.

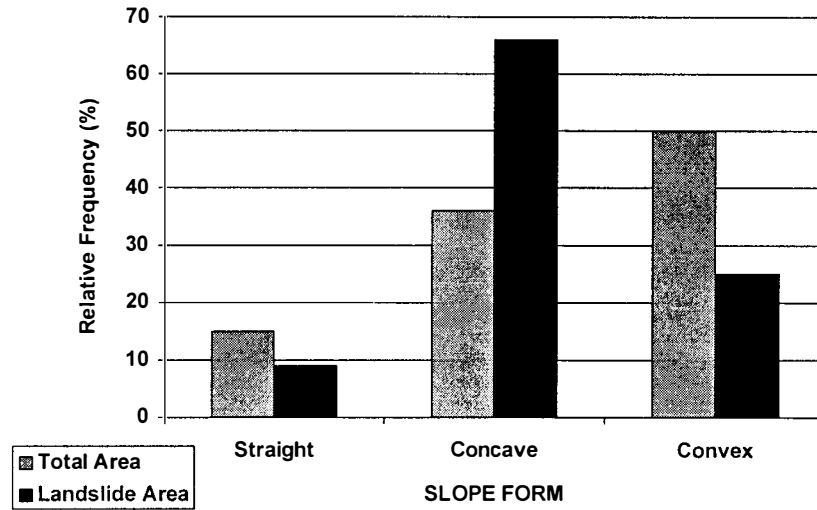
on dip slopes due to percolation along bedding planes, which can generate excessive pore pressures (Carson and Kirkby, 1972). Similarly, at Webb Mountain, just northeast of the study area, Koch (1974) related the high incidence of failure on south slopes to the southerly dip direction.

Slope Form

Figures 19 and 20 show the relative frequency and failure rates of the various slope forms in each attribute class. The most common slope form in plan form (cross section) is convex, while concave profile forms were slightly more prevalent than convex. Clark (1987) also found that a slightly to moderately concave profile was prevalent in the Appalachians. Straight slopes in plan or profile are the least common. In profile, straight slope segments tend to be overtaken by the upslope extension of basal concavity and the downslope encroachment of the upper convex section (Carson and Kirkby, 1972). In cross section, concave slopes have the highest failure rates in the study area. This finding agrees with studies by Bogucki (1970), Aniya (1985), Ryan (1989), and Gao (1993).

When considering the importance of slope concavity or hollows on debris slide susceptibility, it is important to examine the question of the genesis of hollows. Whether or not concavity in hillslope cross sections is caused by debris sliding or by some other geomorphic processes is a matter of debate. According to Moore et al. (1991), low order stream channels can be initiated by

(a) SLOPE PLAN FORM :
Relative Frequency



(b) SLOPE PLAN FORM :
Failure Rate

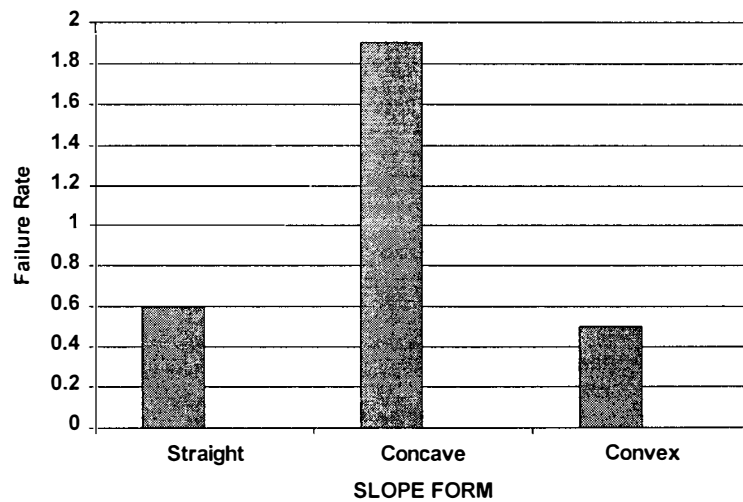
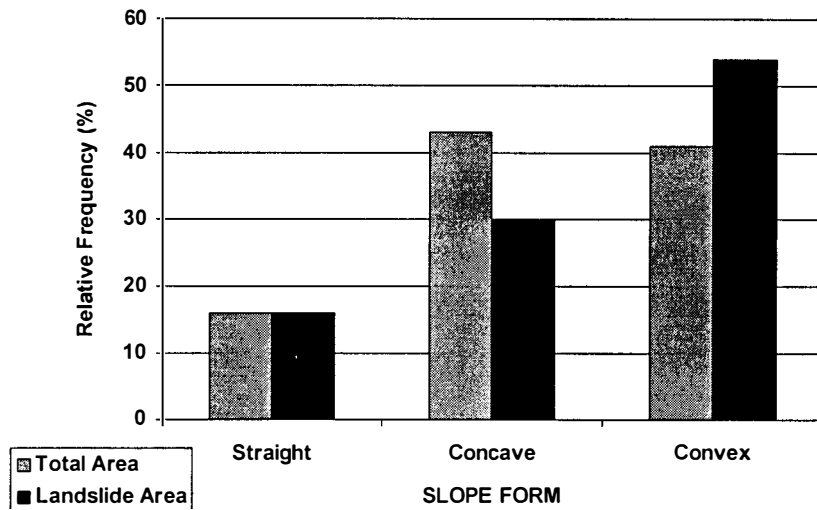


Figure 19. Relative Frequency and Failure Rate for Slope Plan Form.

(a) SLOPE PROFILE FORM :
Relative Frequency



(b) SLOPE PROFILE FORM :
Failure Rate

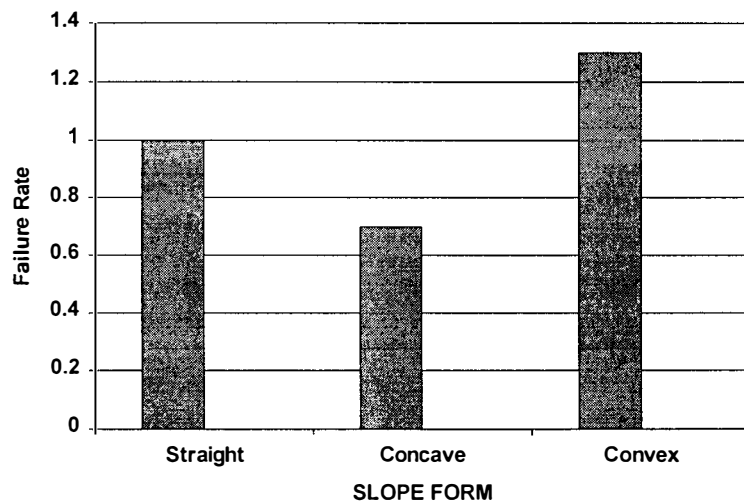


Figure 20. Relative Frequency and Failure Rate for Slope Profile Form.

four processes: incision by Hortonian overland flow, incision by saturated overland flow, seepage erosion, and shallow landsliding. Ryan (1989) asserts that hollow formation on Anakeesta Ridge may be attributed to wedge failures rather than seepage or incision, noting the lack of perennial stream channels and the unlikely occurrence of overland flow on the forested hillslopes (Figure 21). Wolman and Miller (1960) state that landslides commonly form new gullies in exceptional storms, and these gullies continue to grow during moderate storms. Thus, landsliding leaves a lasting imprint on the form of a hillslope. I observed in the field that many hollows, particularly on Anakeesta Ridge, owe their genesis, to some degree, to slide events.

Besides the possible causation of concavity due to debris sliding, in cross section, concave hillslopes tend to have a higher failure rate due to the convergence of water flow in hollows. Surface runoff and subsurface flow converge from the walls of valleys making the slope highly saturated (Gao, 1993). Although failure rates for straight and convex slope forms are considerably less than for those in concavities, the presence of slide-affected areas on these slopes suggests that conditions of elevated pore pressure can be met in areas with little or no topographic convergence. Another plausible explanation is that flow convergence occurred in subtle hollows that are not visible at the level of resolution of the DEM.

In the profile view, the differences are not pronounced, but convex slopes had the highest failure rate overall, followed by

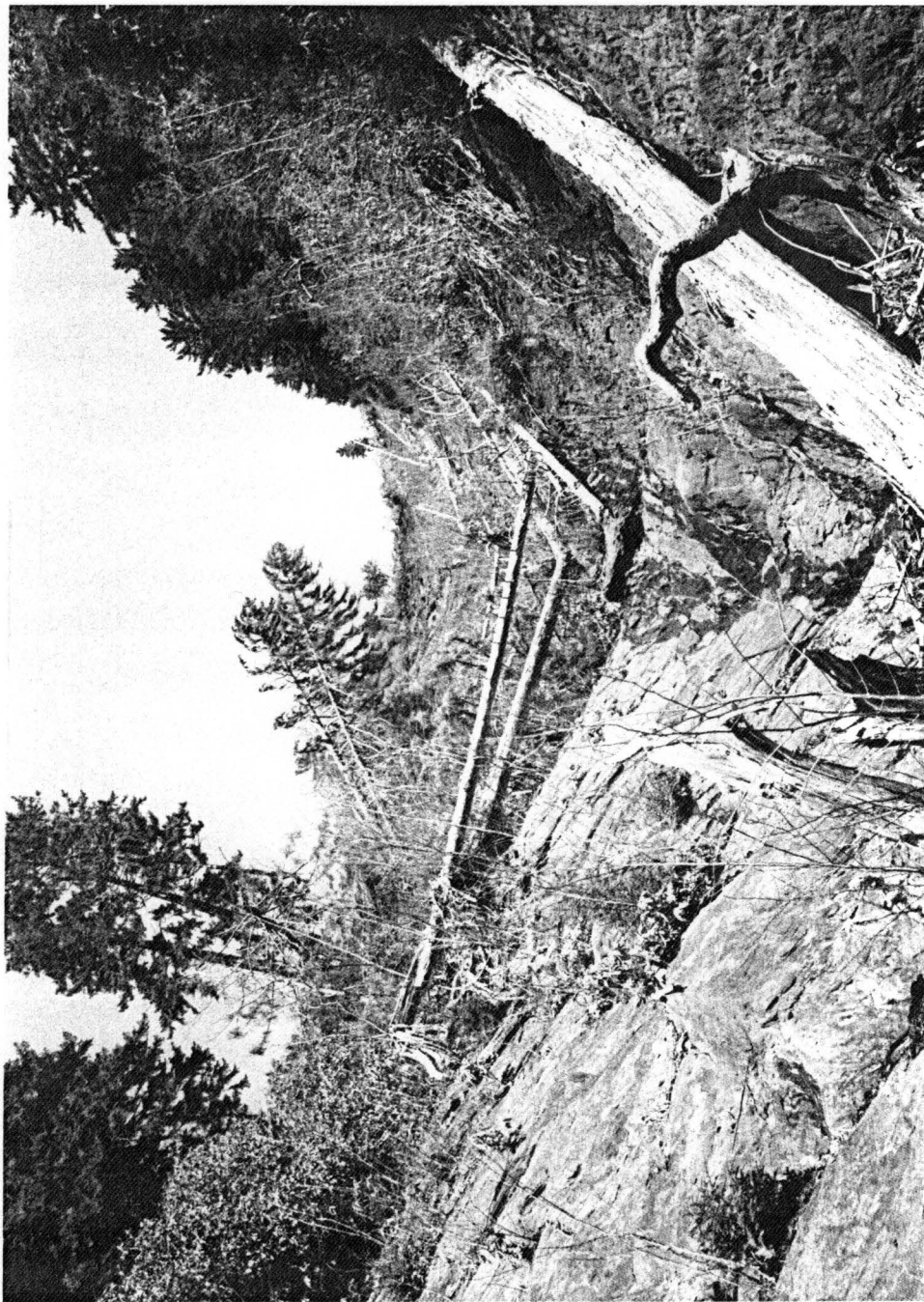


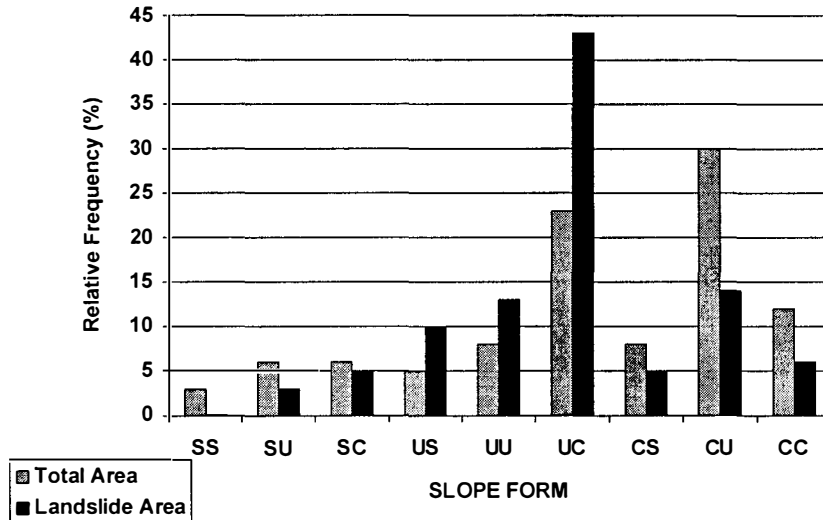
Figure 21. Wedge Failure on Anakeesta Ridge.

straight and concave, respectively. In Gao's (1993) study, concave profiles had a slightly higher failure rate than straight and convex, which were approximately equal. In contrast, Aniya (1985) found that straight slopes in profile were most susceptible to failure near Tokyo, Japan. Differences between these results and those from similar studies indicate that the influence of profile shape on slope stability is not altogether certain, and in fact, is less significant than other local factors.

In profile, convex slopes are unstable due to the slope structure. Unlike concave slopes, convex slopes do not provide the basal support to potential slide masses (Carson and Kirkby, 1972). The concave shape is less important in profile than in cross section because water moves down the profile in a uniform direction as opposed to converging. Straight slope segments may have a fairly significant failure rate (1.0) because they tend to be located just below the upper convex portions of the profile, and scars extend down into the straight portions.

The combinations of plan and profile slope shapes were also examined (Figure 22). Convex/concave (plan/profile) slope forms had the highest frequency in the study area, followed by concave/convex. The slopes with a concave/straight form have the highest failure rate at 2.1, followed by concave/convex and concave/concave shapes, respectively. Combinations of straight or convex plan forms yield low failure rates in general because slides generally occur in hollows rather than noses or straight slope segments. Gao (1993), working in Nelson County, Virginia, found

(a) SLOPE FORM : Relative Frequency



(b) SLOPE FORM : Failure Rate

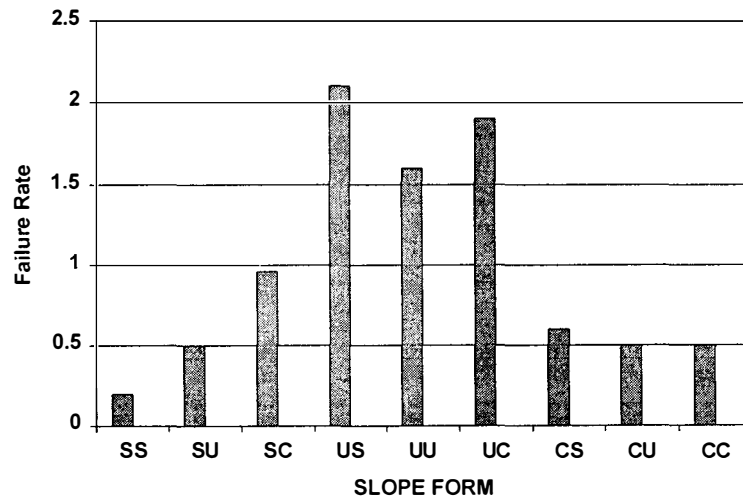


Figure 22. Relative Frequency and Failure Rate for Slope Form. (First letter = shape in plan; second letter = shape in profile. S = straight; U = concave; C=convex)

concave/concave slopes to be most susceptible to failure, with concave/straight second. In Italy, Carrara et al. (1977) also found concave/concave slopes to be highly susceptible. Both the present study and those cited indicate that concave cross sections are very susceptible to landsliding, or, as previously discussed, that concavities may be the result of landslide activity.

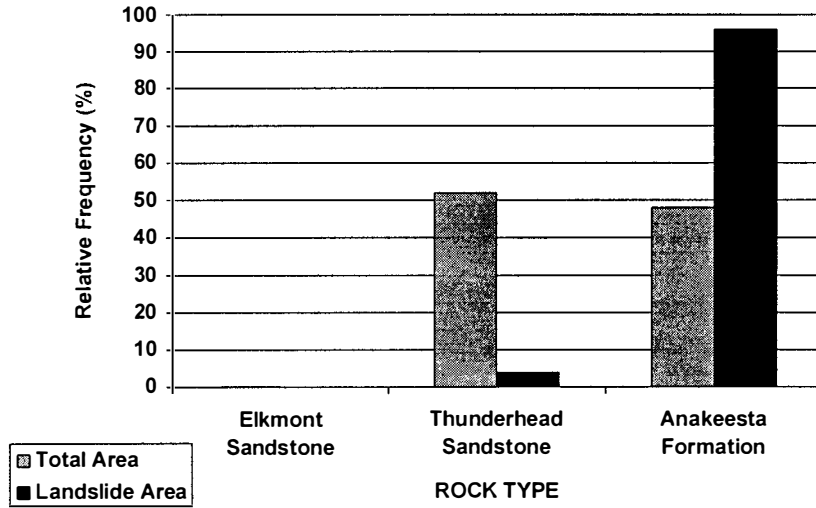
Lithology

Figure 23 shows the relative frequency and failure rates of the three lithologies in the study area. Lithology clearly plays an important role in site location of debris slides. Although Thunderhead Sandstone is the dominant lithology in the area, virtually all the slides (96%) occurred in the Anakeesta Formation, resulting in a high failure rate (2.0).

Compared to the Thunderhead Sandstone, the abundant bedding, joint, and cleavage discontinuities of the Anakeesta Formation provide more failure planes along which slides can be initiated. The slate and phyllite rocks of the Anakeesta are much less cohesive than the thick, coherent Thunderhead Sandstone. Wang (1992), in his studies of mass movements in China, also found that slides were more prevalent in phyllite rocks. Similarly, Gerrard (1994) concluded that phyllite rocks were most susceptible to landsliding in the Himalayas.

Evidently, the particular qualities of the Anakeesta rock types themselves make these slopes susceptible to failure. However, I reasoned that another factor, slope angle, may be

(a) LITHOLOGY : Relative Frequency



(b) LITHOLOGY : Failure Rate

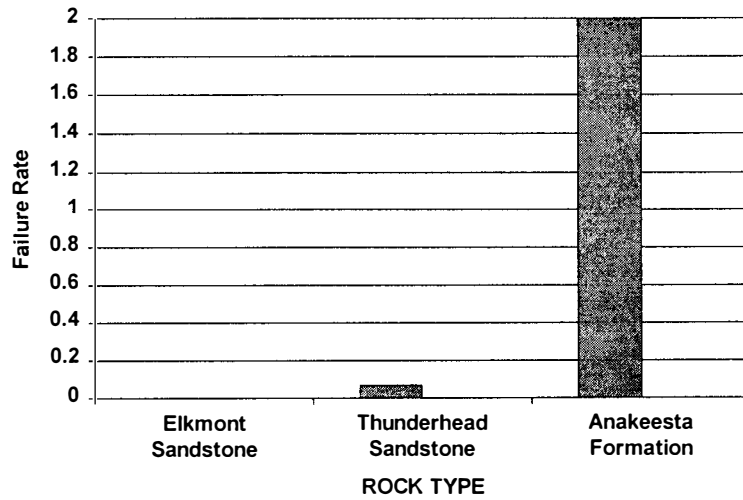


Figure 23. Relative Frequency and Failure Rate for Lithology.

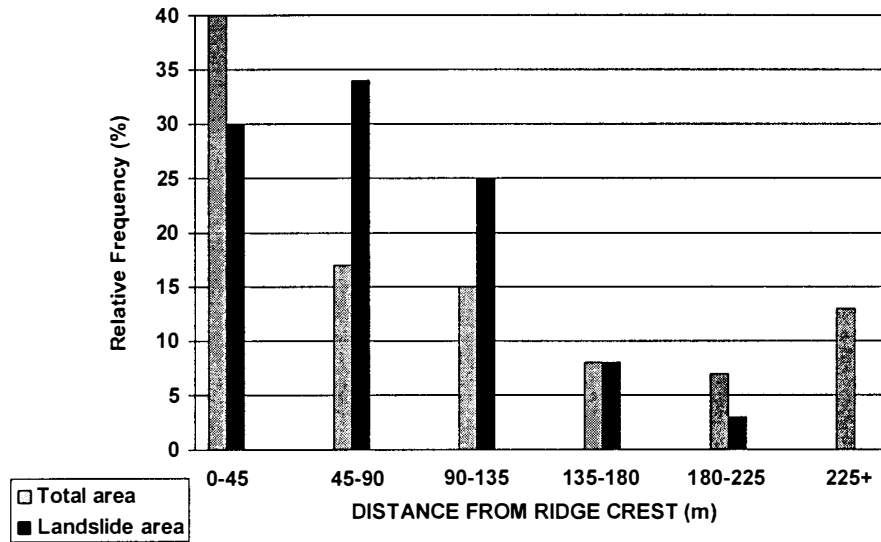
related to lithology, thereby influencing the FR results. Specifically, I wanted to determine whether or not the areas underlain by the Anakeesta Formation had a higher percentage of slopes in the critical slope angle range (36-50+ degrees) than the Thunderhead Sandstone. The abundance of pre-established planes of failure in the Anakeesta Formation seems to have an important role in determining hillslope gradients. Results show that there is a slightly higher percentage of slopes in the critical range in the Anakeesta (51 percent) when compared to Thunderhead Sandstone (48 percent). However, this small difference is insufficient to account for the large difference in failure rate between these formations. Hillslopes underlain by Thunderhead Sandstone exhibit steep slopes due to its resistance and corresponding tendency to develop steep bluffs. In contrast, hillslopes underlain by the Anakeesta Formation exhibit steep gradients due to the coincidence between slope orientation and structural discontinuities.

Distance to Ridge Crest

Figure 24 displays the relative frequency and failure rates in the categories of distance to ridge crest variable. Over 40 percent of the area is within 45 m of a ridgeline. This indicates a large number of ridge lines crisscrossing the area.

The highest failure rate is in the zone 45-90 m from the ridge crest. Aniya (1986) determined that the failure rate is greatest in the 60-80 m class, which is within the range of these findings. No

**(a) DISTANCE FROM
RIDGE CREST : Relative Frequency**



**(b) DISTANCE FROM
RIDGE CREST : Failure Rate**

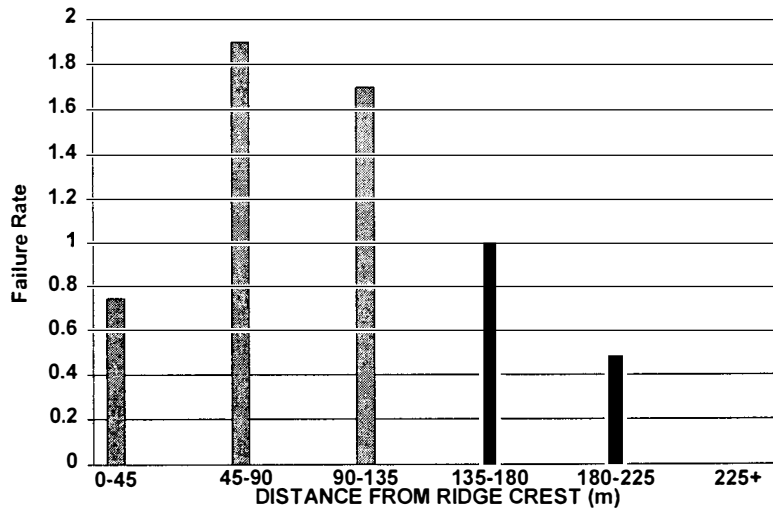


Figure 24. Relative Frequency and Failure Rate for Distance from Ridge Crest.

failures occurred at a distance greater than 225 m from the ridge crest. Only in the range between 45-180 m from the ridge was there a failure rate greater than 1.

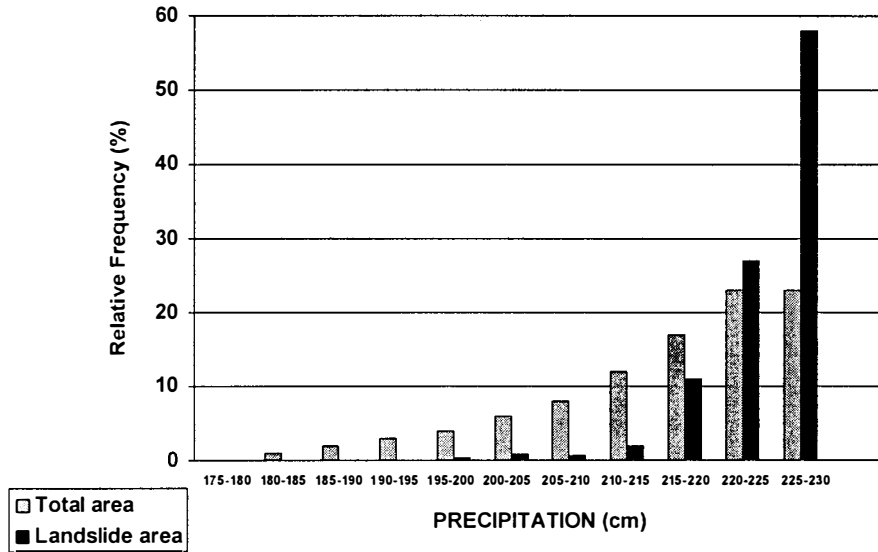
The failure rate is less than 1 in the range 0-45 m presumably because there is an insufficient accumulation of flow in this area in close proximity to the ridge line. Failure rates are highest at an intermediate position because more flow accumulates as the size of the contributing area increases. Moreover, the section of the hillslope just below the upper convexity tends to be steep so that the minimum distance from ridge may be dictated by the local ridge crest convexity and not hydrologic effects. The incidence of landslides falls off at a certain distance from the ridge line probably because the slope angle gets lower at these distances.

Although areas within 45 meters of a ridge were disturbed by landslides, continuous backwasting at the scarhead in the direction of the ridge has expanded the extent of some scars beyond their original form (Figure 7). The location of head scarps during the initial failure may have been much farther downslope. Therefore, these scar areas close to ridge crests may not represent the location of the original, catastrophic event.

Precipitation

Figure 25 shows the relative frequency and failure rates for the precipitation variable. According to failure rate analysis, precipitation appears to be one of the most important contributors to slope instability in the study area. The precipitation class

(a) PRECIPITATION : Relative Frequency



(b) PRECIPITATION : Failure Rate

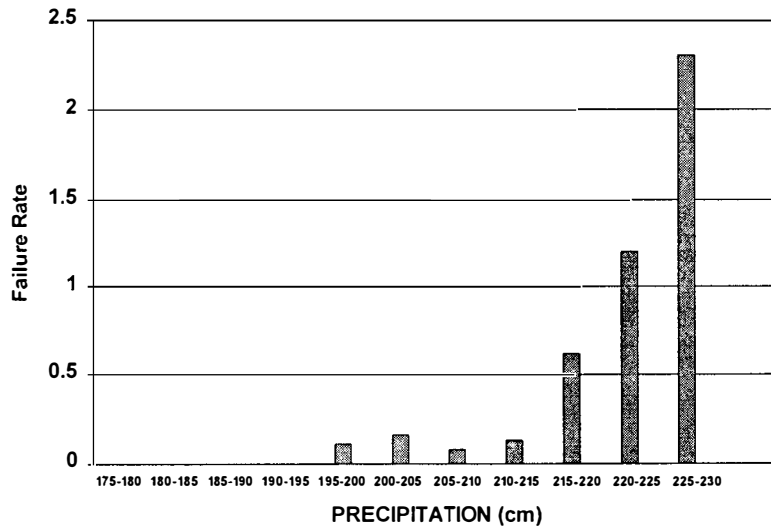


Figure 25. Relative Frequency and Failure Rate for Total Annual Precipitation.

between 225-230 cm had the highest failure rate and was also the class representing maximum annual precipitation totals in the study area. It is interesting to note that failure rates are zero below 195 cm annual precipitation. Recalling that precipitation values were derived from elevation, the 195 cm total roughly corresponds to an elevation of 1200 m. Shanks (1954) found that a water surplus exists throughout the year above 1158 m (3800 ft), which is relatively close to 1200 m. Moreover, most of the intense rainfall occurs above 1219 m (4000 ft) (Shanks, 1954; Bogucki, 1970). Therefore, surplus moisture and/or intense rainfall seem to be very important in debris slide susceptibility in this area.

The strong influence of the precipitation variable on slope instability may have some relation to temperature differences. As precipitation totals increase in the study area, temperatures tend to decrease because the temperature is negatively correlated with elevation. Lower temperatures at high elevations probably increase freeze-thaw action, decreasing the strength of slope materials and weakening pre-established failure planes in discontinuities, particularly those in the Anakeesta Formation. Lower temperatures also decrease evapotranspiration rates. Colder temperatures may thereby contribute to instability at high elevations, where annual precipitation is greatest.

Another reason that precipitation seems to play a major role in slope failures again relates to the correlation between precipitation and elevation. In the study area, the higher elevations are dominated by the Anakeesta Formation. The Anakeesta

Formation is much more prone to failure than Thunderhead Sandstone. The Anakeesta Formation is found at high elevation because it is at the top of the stratigraphic sequence in this section of the GSMNP. The Pearson correlation between precipitation and the presence of Anakeesta grid cells is approximately .5, the highest correlation between any two of the variables. Above 1500 m, the Anakeesta Formation underlies 65% of this area, while for the study area as a whole, the Anakeesta underlies only 47%.

Debris Slide Susceptibility Map

The debris slide susceptibility map created by failure rate analysis with separation into four susceptibility zones is shown in Figure 26. A second susceptibility map is provided in Figure 27 in which a continuous shading was applied through the full range of failure rate values for all grid cells. The amount of area covered by each category is shown in Table 4. Ninety-four percent of the existing debris slide cells were located in medium and high

Table 4. Failure Rate Susceptibility Map Results.

INSTABILITY ZONE	CELL COVERAGE	DEBRIS SLIDE CELLS	PERCENT*
Very Low	11814	2	>1
Low	32615	23	5
Medium	20600	159	37
High	3403	244	57
Total	68432	428	100

*Represents percent of total debris slide cells.

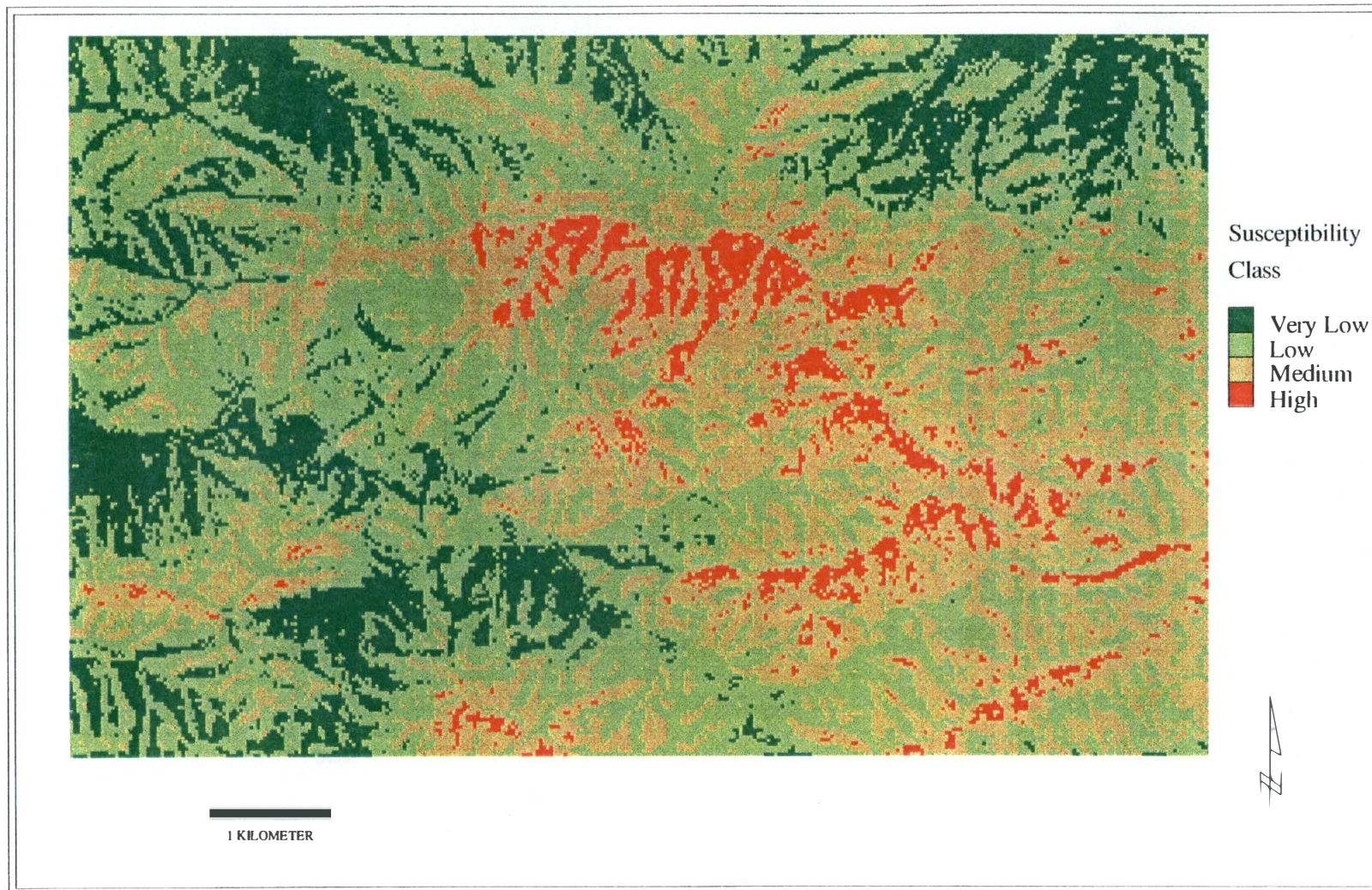


Figure 26 . Map of Debris Slide Susceptibility Zones Determined by Failure Rate Analysis .

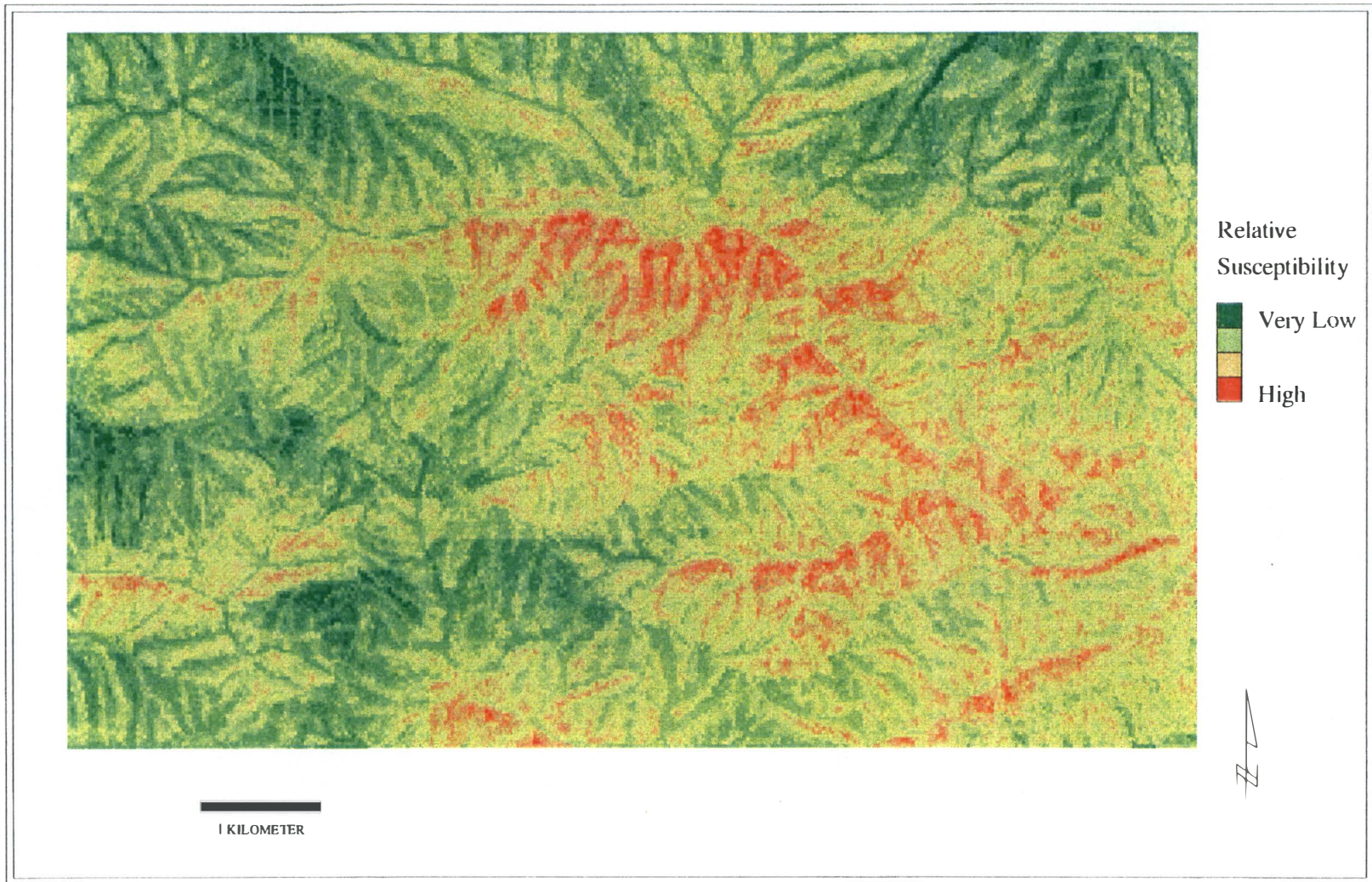


Figure 27. Map of Debris Slide Susceptibility Determined using Failure Rate Analysis and Printed using Continuous Shading.

susceptibility zones. Only one slide, representing less than one percent of the total slide affected areas, was located totally outside the medium-high susceptibility zones. This slide is at a lower elevation and also is oriented to the northeast; both of these attributes are uncommon in slides in this area. This slide was probably not affected by anthropogenic factors because it is not near a road or trail. However, this slide did occur in a hollow on a steep slope of the Anakeesta Formation; both of these conditions contribute to instability in this area.

Logistic Regression Analysis

The goal in the logistic regression analysis was to identify the independent variables that were most important to debris slide susceptibility and to establish a logistic regression equation that expressed this relationship. Then, as with failure rate analysis, debris slide susceptibility per cell could be mapped. Numerous iterations were executed that incorporated various combinations of independent variables. A forced entry of all variables was executed, and the change in prediction power of the regression equation was noted as variables were systematically removed. In the final outcome, certain variables were retained while others were eliminated altogether due to their lack of importance statistically. I will first examine the performance of individual variables. Then, I present the final regression equation used to produce the debris slide susceptibility map.

Slope angle was significant at the .00 level in all iterations, and when individually regressed against the dependent variable, ranked fifth in prediction power. Some correlation exists (.3) between slope angle and precipitation, probably because of the relationship between precipitation and elevation. The lower elevations in the western portion of the study area are in valleys and tend to have lower hillslope gradients than at high elevations.

Four vectors were used to represent slope aspect. Difference in degrees from south, east, and direction of dip were entered into the analysis, along with a fourth vector obtained by multiplying the south and east vectors together. The vector representing difference from east was not significant, and there was no interaction noted in the combined south and east vector. The vectors representing difference from south and difference from dip were approximately equal in importance. Because aspect seems to be important as it relates to difference in degrees from the dip direction, the difference from dip vector was incorporated into the final equation. When the "dip" vector was individually regressed against the dependent variable, this variable ranked first in prediction power among all variables.

With regard to slope form, both plan and profile variables were significant in general, although profile was always less significant. Individually, the plan and profile variables ranked fourth and sixth, respectively, in prediction power. The profile variable was eliminated from the final equation because, without

this variable, the overall regression equation loses a very small amount of prediction power (.5 percent).

The lithology variable, which represents the presence or absence of the Anakeesta Formation in the grid cell, was highly significant (.00) in all iterations. When regressed individually, lithology ranked second in prediction power among variables. Significant correlation (.5) exists between lithology and the precipitation variable.

The distance from ridge crest variable, while significant at the .00 level when regressed against the dependent variable, was only significant at the .1 level when combined with all other variables. In addition, the variable did not add any worthwhile prediction power to the final regression equation. Hence, the distance to ridge crest variable was eliminated. Perhaps a more descriptive variable such as percent distance between ridge crest and valley might have been more descriptive.

Precipitation was likewise highly significant (.00) in all iterations. This variable ranked third in prediction power among independent variables regressed individually against the debris slide variable. That precipitation correlates fairly highly with lithology (.5 Pearson) probably accounts for some of its importance, but precipitation is definitely significant, in and of itself.

The final regression equation computed using all available variables is:

$$p = \frac{1}{1 + e^{-z}}$$

where Z is the linear combination of:

$$Z = -18.24 + .0920X_1 + 2.0581X_2 - .7699X_3 + .1998X_4 + .0192X_5$$

- where X_1 = slope angle
- X_2 = presence/absence of Anakeesta
- X_3 = slope plan form
- X_4 = precipitation
- X_5 = degree difference from dip

The signs of the coefficients do not provide any useful information unless all the independent variables are independent, which is not the case with these factors.

Table 5 lists the five independent variables in the final equation and displays two measures of their relative importance

Table 5. Logistic Regression Statistics for Key Variables.

VARIABLE	PREDICTION POWER	R STATISTIC
Difference from Dip	76	.2579
Anakeesta (Presence/Absence)	73	.1968
Slope Plan Form	67	-.1989
Slope Angle	66	.1748
Precipitation	69	.1318

statistically. The first value, prediction power, represents the percentage of existing debris slide cells correctly predicted when each independent variable is regressed individually against the dependent variable. The R statistic reflects the partial contribution of the variable to the overall model described by the final regression equation (Norusis, 1992). The larger the R statistic, the more important is the variable's contribution to the model. The variables are rank ordered by the value of the R statistic. The only variable in which the magnitude of the R statistic is not comparable with its prediction power is precipitation; this is because much of the information in the precipitation variable is already available to some extent in the "Anakeesta" variable for reasons mentioned previously.

Debris Slide Susceptibility Map

The map produced by logistic regression and reflecting four instability zones is in Figure 28. The amount of area covered by each zone is displayed in Table 6. In a second map, provided in

Table 6. Logistic Regression Susceptibility Map Results.

INSTABILITY ZONE	CELL COVERAGE	DEBRIS SLIDE CELLS	PERCENT*
Very Low	44477	22	5
Low	10279	34	8
Medium	8022	79	18
High	5654	293	68
Total	68432	428	100

* Represents percent of total debris slide cells.



Figure 28. Map of Debris Slide Susceptibility Zones Determined by Logistic Regression.

Figure 29, a continuous shading was applied through the full range of probability values (0-100) for all grid cells. Eighty six percent of the debris slide cells fall into the medium and high susceptibility zones, with over 50% in the high probability category.

Comparison of Methods and Resulting Maps

The two methods used to establish a debris slide susceptibility model, failure rate analysis and logistic regression, are fairly consistent in identifying the independent variables important to debris slide susceptibility. Both techniques revealed some form of the aspect variable to be the most important. Lithology, precipitation, slope angle, and slope plan form were also shown to be highly ranked or significant variables contributing to instability.

Each analysis technique has its own advantages. The results indicate that failure rate analysis is more successful as it assessed over 94% of the observed debris slide areas into medium and high probability ranges, while logistic regression classified only 86% into those ranges. However, logistic regression accomplished the classification with fewer cells in medium and high susceptibility ranges (13676 cells versus 24003 cells in logistic regression and failure rate, respectively). Even though failure rate appears to be more successful in cell classification, logistic regression is more conservative and is less likely to mis-classify a cell as highly susceptible to slope failure.



Figure 29. Map of Debris Slide Susceptibility Determined using Logistic Regression and Printed using Continuous Shading.

A primary difference between the two techniques is the use of categorical variables in failure rate analysis as opposed to scalar variables in logistic regression. Categorization results in the loss of information. Moreover, many subjective decisions have to be made concerning the number categories and the limits to be placed on each. A particularly troublesome decision is involved in separating straight slope forms from those that are convex or concave. Therefore, the logistic regression equation is more objective.

The results of using categorical variables versus scalar values are evident in the two maps. When the maps are separated into stability zones (Figures 26 and 28), the pattern depicted on the failure rate map appears on initial inspection to provide more detail. Large patches of cells in the high susceptibility zone on the logistic regression map show no distinction between small hollows and noses. However, further examination of Figures 27 and 29 (continuous shade maps) shows that, while the general patterns are similar, the logistic regression map exhibits crisper detail in defining slope shape; ridge lines and hollows can be distinguished more clearly than in the failure rate map. These differences in slope form have proven to be critical in both analysis techniques. Therefore, depending upon the arbitrary limits placed on the boundaries between susceptibility zones, a map can appear either very descriptive or highly generalized.

From the viewpoint of ease of understanding for planners and the general public, I believe that the failure rate technique has a

slight advantage. The landslide specialist using these maps must fully understand how a complex GIS map is produced from its computational model of slope stability (Brunsden, 1993), but the mathematics involved in the failure rate technique are relatively simple, such as percent calculations. Understanding logistic regression, however, requires a knowledge of the statistical concept of logit probability, and the resulting formula is relatively more complex.

In terms of providing a graphical interpretation of the influence of variables by class, the failure rate technique has the advantage, even though any categorization simplifies the processes being examined. Categorization allows each class to be ranked within the variable itself and against all other variables. However, the rankings produced by failure rate analysis do not account for relationships between individual variables. Logistic regression, on the other hand, allows for the examination of interrelationships between independent variables and also supports the ranking of variables in terms of relative importance in explaining debris slide occurrence.

Weighing the merits of both techniques, I conclude that logistic regression is preferable to failure rate analysis in debris slide susceptibility studies. In logistic regression, information is not lost through categorization and the resulting map more accurately represents the values for each grid cell, based on the scalar values entered into the regression equation. Logistic regression also does not require subjective decisions to

establish category boundaries. Future studies should abandon categorization in favor of scalar analysis, as the processing power of currently available GIS and statistical packages accommodates larger data sets.

Limitations of Landslide Susceptibility Maps

The maps produced in this study provide useful information for slope failure analysis over a large area; yet, the products have limitations. My maps display debris slide susceptibility in general terms, showing areas with relative probabilities for failure. The determination of actual temporal probabilities requires an analysis of triggering factors, such as rainstorms or winds of a specific intensity in relation to landslides. In most cases, it is extremely difficult to quantify the relationship between these triggering factors and landslides (Mantovani et al., 1996). Future studies in this area should focus on establishing temporal prediction capabilities.

Another disadvantage to these maps is the resolution of the data. Accuracy and resolution of the topography are especially important in steep, finely dissected terrain where debris flows are important processes (Montgomery and Dietrich, 1994). Although 30 m resolution has been used in landslide susceptibility studies over a large area, much information is lost due to the cell size. The subtleties of the landscape are not captured with large cell sizes due to the inherent smoothing of the topography. For more site specific endeavors, a finer resolution is a necessity.

Nonetheless, for mapping a study area of this size, I found that the 30 m cell size is sufficient to delineate slide scars and examine the independent variables in sufficient detail to establish definite relationships.

A third problem that I encountered was that of determining the extent of the slide path to be digitized for analysis. It is important to delineate the area in which failure of the mass was initiated, the primary site of instability. However, there is some dispute as to whether failure is initiated at midslope or at the scar head (Bogucki, 1970; Ryan, 1989). Therefore, I digitized the existing slides from at least the midslope to the scar head to encompass the full range of the area which may have failed. The size of the scar nearest the head constituted the largest portion of the total slide area, so the analysis is probably biased toward the upper slide area. An alternative technique is to digitize the slides as point locations at midslope, but I chose to use polygons to more closely duplicate the actual features.

Fourth, most of the debris slides on the south slope of Mount Leconte resulted from an extremely intense, highly localized cloudburst in 1951 (Bogucki, 1970). The result was a clustering of debris slides on a southerly aspect within a limited portion of the study area. The localized nature of the storm may have biased the results toward placing a very high importance on south aspects. On the other hand, the importance of the direction of dip may be sufficient to explain the predominance of southern aspects.

Finally, these maps do not incorporate all of the factors involved in the slope failure process. No study can integrate all factors, as the natural landscape is so complex and the possible mechanisms so varied that landslide description is a notorious academic problem (Brunsden, 1993). The research could have incorporated the engineering approach to slope stability analysis, which provides precise, site-specific measurements of physical-chemical soil and rock properties as measured in laboratory and field tests. Future trends in susceptibility analysis will combine engineering approaches with broad-scale studies by including some soil mechanics into the factor mapping programs (Brunsden, 1993), but the need to generalize these site characteristics over space in mountain regions will continue to limit their contributions to studies of this scale.

CHAPTER VII

SUMMARY AND CONCLUSIONS

This work is the first known application of debris slide susceptibility mapping in the Great Smoky Mountains National Park. The research has demonstrated the capabilities of computer analysis in debris slide susceptibility mapping and two techniques for analyzing a number of contributing factors over a large area. In addition, the analysis has helped further our understanding of debris sliding in the National Park. This project has produced two maps of debris slide susceptibility in the Great Smoky Mountains National Park. However, the models used to produce the maps are only valid in regions characterized by similar geological, geomorphological and climatic settings. For each land system, a different model is required that reflects the specific and sometimes unique conditions leading to slope failure (Carrara et al., 1991).

The two methods used to establish a debris slide susceptibility model, failure rate analysis and logistic regression, have their own unique merits and deficiencies. Although failure rate analysis allows for an easily understandable graphical representation, this technique requires many subjective decisions regarding categorical subdivisions of variables. Logistic regression, however, provides a more accurate assessment of individual cell susceptibility because no information is lost

through categorization when scalar variables are used. Both techniques offer methods of ranking the relative importance of individual variables.

The analysis shows that debris slides are more common on south facing slopes, which in this study area are the dip slopes. While some studies have found that instability is greater on north facing slopes due to the greater amount of available moisture at these slope aspects, the prevailing direction of dip seems to be the controlling factor in determining the compass direction most susceptible to failure in this study area.

Slope failure is also strongly related to precipitation. Areas where total annual precipitation is highest in the study area are much more susceptible to failure than areas with relatively low precipitation totals. The importance of precipitation to slope instability in this area appears due, at least in part, to the correlation between increased precipitation and the prominence of the Anakeesta Formation at high elevations; however precipitation has been shown to be an important variable in and of itself.

Slopes underlain by the Anakeesta Formation, with its dense jointing and cleavage, are much more apt to fail than those on other lithologies. Notwithstanding the aforementioned correlation with precipitation, the structural discontinuities in the Anakeesta appear to be the major contributor to its instability.

With regard to slope form, concave cross sections are most favorable to slope failure, presumably because of the convergence of water flow in hollows. Many of these hollows doubtless owe

their genesis to debris slides, particularly those which begin as wedge failures. Differences in slope form in profile did not prove to be an important factor in assessing slope instability.

The majority of slides occurred where slope angles ranged between 30 and 50 degrees. On slopes underlain by the Anakeesta Formation, existing slope angles were probably defined by debris slides, themselves.

Lastly, the variable representing distance from ridge crests was not especially significant and was eliminated in the logistic regression procedure. Failure rate analysis indicated that a distance from ridge crest between 45-90 m has the highest susceptibility to fail.

Despite the fact that landslides are generally more predictable than earthquakes, volcanic eruptions, and some storms, it is still virtually impossible to forecast the location, magnitude, and timing of specific future landslide events (Brabb, 1991; Jones, 1992). The complex interrelationships of numerous factors that vary over space and time make slope stability assessment a difficult endeavor. Unfortunately, this lack of precision has caused some planners and politicians to lose interest in efforts to map landslide prone areas (Jones, 1992).

Still, susceptibility mapping, when integrated into the planning process, can definitely reduce losses due to landslides. Potential costs of failure may be several orders of magnitude greater than the costs of investigation (Jones, 1992). Moreover, with improvements in computer hardware and software packages,

landslide susceptibility analysis is becoming an increasingly more straightforward process when the required data are available. The boost given to GIS by these improvements is probably going to increase the number of users of this technology for slope instability mapping at a rapid rate (Brunsden, 1993). With GIS technology, planners and decision makers can receive understandable hazard maps much more easily and cheaply than with manual methods, thus facilitating the transfer of knowledge from earth scientists to the general public (Dikau et al., 1996).

Therefore, a greater emphasis is needed by decision makers on landslide susceptibility mapping. Landslide inventory maps that show where landslides have occurred probably cover less than one percent of the land and sea areas of the world (Brabb, 1991). Recognizing this deficiency, UNESCO has placed hazard, risk, and susceptibility mapping at the center of active research programs in landslide prone areas of the world (Brunsden, 1993). As anthropogenic activities continue to expand into mountainous areas, this type of information becomes critically important to adequate planning.

This study has demonstrated the utility of Geographic Information Systems in landslide studies. Despite its usefulness, the implicit reliance on GIS to provide information to adequately construct physically-based models should be avoided. Uncertainty in spatial modeling can only in part be solved by advanced computer technologies. I am in agreement with Dikau, Cavallin, and Jager

(1996), that computer technology must be buttressed by the continuation of classical, field-based landslide research.

Nonetheless, landslide researchers should definitely make use of computer capabilities because of their ability to accommodate very large data sets and display the results of analysis in many different formats. As in this study, researchers must recognize limitations in resolution and other deficiencies. Future studies of landslide susceptibility must focus on incorporating a larger set of variables gleaned from more precise and accurate data sets.

LIST OF REFERENCES

LIST OF REFERENCES

- Aniya, Masamu. 1985. "Landslide Susceptibility Mapping in the Amahata River Basin, Japan." Annals of the Association of American Geographers 75 (1): 102-114.
- Baird, Douglas D. 1990. Wedge Failures in the Blue Ridge Province of East Tennessee: A Case Study of the Hartford Area Slides. Masters Thesis, University of Tennessee, Knoxville.
- Band, L.E., and I.D. Moore. 1995. "Scale: Landscape Attributes and Geographical Information Systems." Hydrological Processes 9: 401-422.
- Bell, F.G. 1983. Fundamentals of Engineering Geology. Butterworth and Company, Boston.
- Bernknopf, Richard L., Russell H. Campbell, David S. Brookshire, and Carl D. Shapiro. 1988. "A Probabilistic Approach to Landslide Hazard Mapping in Cincinnati, Ohio with Applications for Economic Evaluation." Bulletin of the Association of Engineering Geologists 25 (1): 39-56.
- Bogucki, Donald J. 1970. Debris Slides and Related Damage Associated with the September 1, 1951 Cloudburst in the Mt. Leconte-Sugarland Mountain Area, Great Smoky Mountains National Park. Doctoral Dissertation, University of Tennessee, Knoxville.
- Bogucki, Donald J. 1972. "Intense Rainfall in the Great Smoky Mountains National Park." Journal of the Tennessee Academy of Science 47 (3): 93-97.
- Brabb, Earl E. 1989. "Landslides: Extent and Economic Significance in the United States." Pages 25-50 in Brabb, Earl E., and Betty L. Harrod, eds. Landslides: Extent and Economic Significance. A.A. Balkema, Brookfield, Vermont.
- Brabb, Earl E. 1991. "The World Landslide Problem." Episodes 14 (1): 52-61.
- Brundsdon, Denys. 1993. "Mass Movement; the Research Frontier and Beyond; a Geomorphological Approach." Geomorphology 7: 85-128.
- Campbell, Carlos C., Hutson, William F., and Sharp, Aaron J. 1992. Great Smoky Mountain Wildflowers. University of Tennessee Press, Knoxville, Tennessee.

- Carrara, A., M. Cardinali, R. Detti, F. Guzzetti, V. Pasqui, and P. Reichenbach. 1991. "GIS Techniques and Statistical Models in Evaluating Landslide Hazard." Earth Surface Processes and Landforms 16: 427-445.
- Carrara, A., E.P. Carratelli, and L. Merenda. 1977. "Computer-based Data Bank and Statistical Analysis of Slope Instability Phenomena." Zeitschrift fur Geomorphologie 21 (2): 187-222.
- Carson, M. A., and M. J. Kirkby. 1972. Hillslope Form and Process. Cambridge University Press, London.
- Carter, James R. 1988. "Digital Representations of Topographic Surfaces." Photogrammetric Engineering and Remote Sensing 54 (Nov): 1577-1580.
- Chorley, Richard J., Stanley A. Schumm, and David E. Sugden. 1984. Geomorphology. Muethen and Company, New York.
- Clark, G. Michael. 1987. "Debris Slides and Debris Flow Historical Events in the Appalachians South of the Glacial Border." Reviews in Engineering Geology 7: 125-138.
- Clark, G. Michael, Patrick T. Ryan, and Eric C. Drumm. 1987. "Debris Slides and Debris Flows on Anakeesta Ridge, Great Smoky Mountains National Park, Tennessee." Pages 18-19 in Schultz, Arthur P. and C. Scott Southworth, eds. Landslides of Eastern North America. U.S. Geological Survey Circular 1008.
- Crozier, Michael J. 1986. Landslides: Causes, Consequences, and Environment. Croom Helm, Dover, New Hampshire.
- Daily Times, 11 Oct. 1995 , 17 Oct 1995, 14 May 1995.
- Dietrich, William E., Robert Reiss, Mei-Ling Hsu, and David R. Montgomery. 1995. "A Process-Based Model for Colluvial Soil Depth and Shallow Landsliding Using Digital Elevation Data." Hydrological Processes 9: 383-400.
- Dikau, Richard. 1990. "Derivatives from Detailed Geoscientific Maps Using Computer Methods." Zeitschrift fur Geomorphologie 80 (Dec): 45-55.
- Dikau, Richard, Angelo Cavallin, and Stefan Jager. 1996. "Databases and GIS for Landslide Research in Europe." Geomorphology 15: 227-239.
- Environmental Systems Research Institute (ESRI). 1993. Understanding GIS: The ARC/INFO Method. John Wiley and Sons, Inc.

- Environmental Systems Research Institute (ESRI). 1994. Cell Based Modeling with GRID. Environmental Systems Research Institute, Inc., Redlands, California.
- Feldkamp, Susan M. 1984. Revegetation of Upper Elevation Debris Slide Scars on Mount Leconte in the Great Smoky Mountains National Park. Masters Thesis, University of Tennessee, Knoxville.
- Fleming, Robert W. and Fred A. Taylor. 1980. Estimating the Costs of Landslide Damage in the United States. U.S. Geological Survey Circular 832.
- Franklin, Steven E. 1987. "Geomorphometric Processing of Digital Elevation Models." Computers and Geosciences 13 (6): 603-609.
- Gao, Jay. 1993. "Identification of Topographic Settings Conducive to Landsliding from DEM in Nelson County, Virginia, U.S.A." Earth Surface Processes and Landforms 18: 579-591.
- Gerrard, John. 1994. "The Landslide Hazard in the Himalayas: Geological Control and Human Action." Geomorphology 10: 221-230.
- Gryta, Jeffrey J. and Mervin J. Bartholomew. 1987. "Frequency and Susceptibility of Debris Avalanching Induced by Hurricane Camille in Central Virginia." Pages 16-18 in Schultz, Arthur P. and C. Scott Southworth, eds. Landslides of Eastern North America. U.S. Geological Survey Circular 1008.
- Gupta, R. P., and B. C. Joshi. 1990. "Landslide Hazard Zoning Using the GIS Approach - A Case Study from the Ramganga Catchment, Himalayas." Engineering Geology 28: 119-131.
- Hack, John T., and John C. Goodlett. 1960. Geomorphology and Forest Ecology of a Mountain Region in the Central Appalachians. U.S. Geological Survey Professional Paper 347. U.S. Government Printing Office, Washington, D.C.
- Hadley, Jarvis B., and Richard Goldsmith. 1963. Geology of the Eastern Great Smoky Mountains, North Carolina, and Tennessee. Geological Survey Professional Paper 349-B. U.S. Government Printing Office, Washington, D.C.
- Hanson, A. 1989. "Landslide Hazard Analysis." Pages 523-602 in Brunnsden, D., and D. B. Prior, eds. Slope Instability. John Wiley and Sons, New York.

- Harrell, F. E. 1983. "The LOGIST Procedure." Pages 181-202 in Joyner, S. P., ed. The SAS Supplemental Library User's Guide. SAS Institute Inc, Cary, North Carolina.
- Jacobson, Robert B., Elizabeth D. Cron, and John P. McGeehin. 1987a. "Preliminary Results of a Study of Natural Slope Failures Triggered by the Storm of Nov 3-5, 1985, German Valley, West Virginia and Virginia." Pages 11-16 in Schultz, Arthur P. and C. Scott Southworth, eds. Landslides of Eastern North America. U.S. Geological Survey Circular 1008.
- Jacobson, Robert B., John P. McGeehin, and Elizabeth D. Cron. 1987b. "Hillslope Processes and Surficial Geology, Wills Mountain Anticline, West Virginia and Virginia". Pages 31-55 in J. Steven Kite, ed. Research on the Late Cenozoic of the Potomac Highlands.
- Jenson, S.K, and J.O. Dominique. 1988. "Extracting Topographic Structure from Digital Elevation Data for Geographic Information System Analysis." Photogrammetric Engineering and Remote Sensing 54 (Nov): 1593-1600.
- Jibson, Randall W., and D.K. Keefer. 1989. "Statistical Analysis of Factors Affecting Landslide Distribution in the New Madrid Seismic Zone, Tennessee and Kentucky." Engineering Geology 27: 509-542.
- Jones, D.K.C. 1992. "Landslide Hazard Assessment in the Context of Development." Pages 117-141 in McCall, G. J. H., D. J. C. Laming, and S. C. Scott, eds. Geohazards: Natural and Manmade. Chapman and Hall, New York.
- King, Phillip B., Jarvis B. Hadley, Robert B. Neuman, and Warren Hamilton. 1958. "Stratigraphy of the Ocoee Series, Great Smoky Mountains, Tennessee and North Carolina." Geological Society of America Bulletin 69 : 947-966.
- King, Phillip B., Robert B. Neuman, and Jarvis B. Hadley. 1968. Geology of the Great Smoky Mountains National Park, Tennessee and North Carolina. Geological Survey Professional Paper 587. U. S. Government Printing Office. Washington, D.C.
- King, Philip B., and Arthur Stupka. 1950. "The Great Smoky Mountains - Their Geology and Natural History." The Scientific Monthly 71 (July): 31-43.
- Knoxville News Sentinel. 6 Oct 1995, 7 Oct 1995.
- Koch, Carl A. 1974. Debris Slides and Related Flood Effects in the 4-5 August 1938 Webb Mountain Cloudburst: Some Past and Present Environmental Geomorphic Implications. Masters Thesis, University of Tennessee, Knoxville.

- McKean, J., S. Buechel, and L. Gaydos. 1991. "Remote Sensing and Landslide Hazard Assessment." Photogrammetric Engineering and Remote Sensing 57 (Sept): 1185-1193.
- Mantovani, Franco, Robert Soeters, and C.J. Van Westen. 1996. "Remote Sensing Techniques for Landslide Studies and Hazard Zonation in Europe." Geomorphology 15: 213-225.
- Moon, B.P. 1986. "Controls on the Form and Development of Rock Slopes in Fold Terrain." Pages 225-243 in A.D. Abrahams, ed. Hillslope Processes. Allen and Unwin Incorporated, Boston.
- Moore, Harry L. 1988. A Roadside Guide to the Geology of the Great Smoky Mountains National Park. University of Tennessee Press, Knoxville, Tennessee .
- Moore, Harry L. 1997. Geologist, Tennessee Department of Transportation, Knoxville, Tennessee. Personal communication, March 10.
- Moore, I.D., R.B. Grayson, and A.R. Ladson. 1991. "Digital Terrain Modelling: A Review of Hydrological, Geomorphological, and Biological Applications." Hydrological Processes 5 : 3-30.
- Montgomery, David R., and William E. Dietrich. 1994. "A Physically Based Model for the Topographic Control of Shallow Landsliding." Water Resources Research 30 (4): 1153-1171.
- Nabors, Pamela J. 1996. The Current Status and Potential Spread of an Invasive Exotic Species: Chinese Yam in the Great Smoky Mountains National Park. Masters Thesis: University of Tennessee, Knoxville.
- National Climatic Data Center. 1995. "Hurricane Opal." Technical Report 95-02. National Climatic Data Center, Asheville, North Carolina.
- Neary, D.G. and L.W. Swift, Jr. 1987. "Rainfall Thresholds for Triggering a Debris Avalanching Event in the Southern Appalachian Mountains." Reviews in Engineering Geology 7: 81-92.
- Newman, Evelyn B., Arthur R. Paradis, and Earl E. Brabb. 1978. Feasibility and Cost of Using a Computer to Prepare Landslide Susceptibility Maps of the San Francisco Bay Region, California. U.S. Geological Survey Bulletin 1443.
- Norusis, Marija J. 1992. SPSS for Windows Advanced Statistics Release 5. SPSS Incorporated, Chicago.

- Pariseau, W.G. and Barry Voight. 1979. "Rockslides and Avalanches: Basic Principles, Perspectives in the Realm of Civil and Mining Operations." Pages 1-92 in Barry Voight, ed. Rockslides and Avalanches. Elsevier Scientific Publishing Company, Amsterdam.
- Patric, J.H. 1976. "Soil Erosion in the Eastern Forest." Journal of Forestry 74: 671-677.
- Pomeroy, J.S. 1984. Pages 220-221 in Geological Survey Research, Fiscal Year 1981. U.S. Geological Survey Professional Paper 1375.
- Reneau, Steven L., and William E. Dietrich. 1987. "Size and Location of Colluvial Landslides in a Steep Forested Landscape." Erosion and Sedimentation in the Pacific Rim (Proceedings of the Corvallis Symposium, August, 1987). IAHS Publication No. 165.
- Rengers, Nick, Robert Soeters, and Cees J. van Westen. 1992. "Remote Sensing and GIS Applied to Mountain Hazard Mapping." Episodes 15 (1): 36-44.
- Ryan, Patrick T., and G. Michael Clark. 1989. "Debris Slides and Flows on Anakeesta Ridge, Great Smoky Mountains National Park, Tennessee." Abstract of the 15th Annual Scientific Research Meeting, Great Smoky Mountains National Park, May 25-26, Gatlinburg, Tennessee.
- Ryan, Patrick T. 1989. Debris Slides and Flows on Anakeesta Ridge within the Great Smoky Mountains National Park, Tennessee, U.S.A. Masters Thesis, University of Tennessee, Knoxville.
- Schneider, Raymond H. 1973. Debris Slides and Related Flood Damage Resulting From Hurricane Camille, 19-20 August, and Subsequent Storm, 5-6 September 1969 in the Spring Creek Drainage Basin, Greenbrier County, West Virginia. Doctoral Dissertation, University of Tennessee, Knoxville.
- Scott, Ralph C., Jr. 1972. The Geomorphic Significance of Debris Avalanching in the Appalachian Blue Ridge Mountains. Doctoral Dissertation, University of Georgia, Athens.
- Shanks, Royal, E. 1954. "Climates of the Great Smoky Mountains." Ecology 35 (July): 357-360.
- Sharpe, C.F. Stewart. 1938. Landslides and Related Phenomena. Cooper Square Publishers, Inc., New York.

- Shasko, M.J., and C.P. Keller. 1991. "Assessing Large Scale Slope Stability and Failure With a Geographic Information System." Pages 267-275 in Michael Heit and Art Shortreid, eds. GIS Applications in Natural Resources. GIS World Inc., Fort Collins, Colorado.
- Sidele, R.C., and P.K. Terry. 1992. "Shallow Landslide Analysis in Terrain with Managed Vegetation." Pages 289-298 in Walling, D.E., T.R. Davies, and B. Hasholt, eds. Erosion, Debris Flows, and Environment in Mountain Regions. International Symposium of Association of Hydrological Sciences, Chengdu, China.
- Smallshaw, James. 1953. "Some Precipitation-Altitude Studies of the Tennessee Valley Authority." American Geophysical Union Transactions 34 (4): 583-588.
- Soil Survey Staff, 1956. Soil Survey of Sevier County, Tennessee. Series 1945, No.1.
- Strahler, A.N. 1950. "Equilibrium Theory of Erosional Slopes Approached by Frequency Distribution Analysis." American Journal of Science 248: 673-696.
- Tennessee Valley Authority. 1937. Precipitation in the Tennessee River Basin Annual 1937. Tennessee Valley Authority, Knoxville, Tennessee.
- Torbett, Allen, and Patrick Ryan. 1986. "Investigation and Analysis of Rock Slopes." Geotechnical Report 86-2, August 1. Department of Civil Engineering, University of Tennessee, Knoxville.
- U. S. Geological Survey. 1987. Digital Elevation Models: Data Users Guide 5. United States Geological Survey, U.S. Department of the Interior, Reston, Virginia.
- Varnes, David J. 1978. "Slope Movement Types and Processes." Pages 11-33 in Schuster, R. L., and Krizek, R. J., eds. Landslides - Analysis and Control. National Research Council, Highway Research Board Special Report 176.
- Varnes, David J. 1984. Landslide Hazard Zonation: A Review of Principles and Practice. Unesco, Paris, France.
- Wadge, G., A. P. Wislocki, and E. J. Pearson. 1993. "Spatial Analysis in GIS for Natural Hazard Assessment." Pages 332-338 in Goodchild, M. F., B. O. Parks, and L. T. Skyaert, eds. Geographic Information Systems and Environmental Modeling. Oxford University Press.

- Wang, Chenghua, and Tom Wonpei. 1992. "An Index System for Delineating Landslide Regions." Pages 307-314 in Walling, D. E., T. R. Davies, and B. Hasholt, eds. Erosion, Debris Flows, and Environment in Mountain Regions. International Symposium of Association of Hydrological Sciences, Chengdu, China.
- Whittaker, Robert H. 1948. A Vegetational Analysis of the Great Smoky Mountains. Doctoral Dissertation, University of Illinois, Urbana.
- Wieczorek, Gerald. F. 1984. "Preparing a Detailed Landslide Inventory Map for Hazard Evaluation and Reduction." Bulletin of the Association of Engineering Geologists 21 (3): 337-342.
- Williams, Garnett P. and Harold P. Guy. 1973. Erosional and Depositional Aspects of Hurricane Camille in Virginia, 1969. U.S. Geological Survey Professional Paper 804.
- Wolfe, J.A. 1967. Forest Soil Characteristics as Influenced by Vegetation and Bedrock in the Spruce-fir Zone of the Great Smoky Mountains. Doctoral Dissertation, University of Tennessee, Knoxville.
- Wolman, M. Gordon, and John P. Miller. 1960. "Magnitude and Frequency of Forces in Geomorphic Processes." Journal of Geology 68: 54-74.
- Zaslavsky, D., and G. Sinai. 1981. "Surface Hydrology: I - Explanation of Phenomena." Journal Hydraulic Division, Proceedings, American Society of Civil Engineers. 107: 1-16.
- Zevenbergen, Lyle W., and Colin R. Thorne. 1987. "Quantitative Analysis of Land Surface Topography." Earth Surface Processes and Landforms. 12: 47-56.

APPENDICES

APPENDIX A - COMPUTER ALGORITHMS.

The following are the computer commands and logic used to create the data layers and calculate the required output.

DATA AVAILABLE. 30 meter DEM, UTM Zone 17, NAD 27, Clarke Spheroid.

SOFTWARE. ARC/INFO GRID.

HARDWARE. Sun workstation.

The study area size is 208 rows x 329 columns. Total number of cells was 68,432.

I. SLOPE ANGLE CALCULATION.

Slope angles for each cell were determined using the SLOPE command applied to the DEM. This command calculates the maximum rate of change in value from each cell to its neighbors. The SLOPE function fits a plane to the elevation values of a 3 x 3 cell window around the cell. The algorithm used to calculate slope is:

$$\text{rise/run} = \text{square root} [(dz/dx)^2 + (dz/dy)^2]$$
$$\text{degree slope} = \text{arctan}(\text{rise/run}) * 57.29578$$

where:

$$dz/dx = ((a + 2d + g) - (c + 2f + I)) / (8 * x \text{ mesh spacing})$$
$$dz/dy = ((a + 2b + c) - (g + 2h + I)) / (8 * y \text{ mesh spacing})$$

where a through I represent elevation values in a window:

```
a b c
d e f
g h i
```

(From ESRI, 1994)

To place the cells into a slope category for FR calculations, the cells were subdivided into 11 categories based on a 5 degree slope interval using the SLICE command:

```
slopcat = slice (slopes, eqinterval, 11)
```

II. ASPECT CALCULATION.

Slope aspect is the direction the slope faces. To determine the slope aspect of each cell, the ASPECT command was utilized. This command calculates the down-slope direction of the maximum rate of change in value from each cell to its neighbors (the direction of the slope). Each cell is encompassed by eight

adjacent points. The azimuthal direction was determined for each point by comparing the differences in height between the point in question and the eight neighboring points.

The cells were placed into eight categories using the SLICE command.

```
aspcat = slice (aspects, equinterval, 8)
```

III. SLOPE FORM CALCULATIONS.

The variable for slope form was a combination of profile and plan forms for each cell. The following steps were used to determine this variable:

a. The CURVATURE command was used to produce two output grids of profile and plan form values for each cell, named profileg and plang respectively. The curvature for each cell is calculated by determining the relationship of the cell to its eight neighboring cells. For each cell, a fourth order polynomial of the form:

$$Z = Ax^2y^2 + Bx^2y + Cxy^2 + Dx^2 + Ey^2 + Fxy + Gx + Hy + I$$

is fit to the interior grid point of a moving 3 x 3 cell window (Zevenbergen and Thorne, 1987; Moore, et al., 1991). The surface defined by the equation passes exactly through the nine submatrix elevations. The coefficients are expressed solely as functions of the grid point elevations and grid spacing. The relationships between the coefficients and the nine values of elevation for each cell in the window are as follows:

$$\begin{aligned} A &= [(Z_1 + Z_3 + Z_7 + Z_9)/4 - (Z_2 + Z_4 + Z_6 + Z_8)/2 + Z_5]/L^4 \\ B &= [(Z_1 + Z_3 - Z_7 - Z_9)/4 - (Z_2 - Z_8)/2]L \\ C &= [(-Z_1 + Z_3 - Z_7 + Z_9)/4 + (Z_4 - Z_6)]/2L^3 \\ D &= [(Z_4 + Z_6)/2 - Z_5]L^2 \\ E &= [(Z_2 + Z_8)/2 - Z_5]/L^2 \\ F &= (-Z_1 + Z_3 + Z_7 - Z_9)/4L^2 \\ G &= (-Z_4 + Z_6)/2L \\ H &= (Z_2 - Z_8)2L \\ I &= Z_5 \end{aligned}$$

where A-I = nine equation parameters

Z = nine submatrix elevations

L = distance between matrix points in the row and column direction

(From Zevenbergen and Thorne, 1987)

Profile curvature is calculated by:

$$\text{plan curvature} = -2 \frac{DG + EH + FGH}{G + H}$$

Plan curvature is calculated by:

$$\text{profile curvature} = 2 \frac{\text{DH} + \text{EG} - \text{FGH}}{\text{G} + \text{H}}$$

(From Moore, et al., 1991)

b. The values for each cell in of profileg and plang were either positive, negative, or zero representing convex, concave, and straight forms respectively. In order to separate each output grid into three classes with discrete values, the following commands were used:

```
FOR PLAN FORM:
  if (plang > 0) curve1 = 3  (convex)
  else if (plang < 0) curve1 = 2  (concave)
  else curve1 = 1  (straight)

FOR PROFILE:
  if (profileg > 0), curve2 = 5  (convex)
  else if (profileg < 0) curve2 = 4  (concave)
  else curve2 = 3  (straight)
```

c. To determine a discrete value for the combination of the two form types, the two grids (curve1 and curve2) were multiplied together, with the resulting number equal to a particular slope form combination. The result of multiplication is nine slope form classes.

PLAN FORM	PROFILE
straight	straight
straight	concave
straight	convex
concave	straight
concave	concave
convex	straight
concave	convex
convex	concave
convex	convex

IV. RIDGE DISTANCE CALCULATIONS:

To determine the distance of each cell to a ridge line, the cells which make up the ridge lines had to first be computed. This was accomplished by first determining the total amount of flow accumulated in each cell from a uniform rainfall across the study area, and assigning cells with zero accumulation to the ridge line group.

a. To determine flow accumulation, the "sinks" in the dem had to be filled using the FILL command. Sinks occur when all eight neighboring cells have elevations higher than the center cell. DEMs almost always contain depressions that hinder flow routing and need to be filled (Jenson and Dominique, 1988). Depressions create problems in determining hydrologic flow directions because they must be filled before flow can continue. Depressions are either removed by smoothing or filling (Jenson and Dominique). Single-cell depressions are filled by raising each cell's elevation to the elevation of its lowest elevation neighbor if that neighbor is higher in elevation than the cell (Jenson and Dominique, 1988). The GRID commands were used to create "filgrid", a sinkless DEM.

Once the "sinks" were filled, the flow direction of water out of each cell was determined using the FLOWDIRECTION command. The direction of flow is assumed to be in the direction of steepest descent from a given node to the eight possible neighboring cells. This is calculated by :

descent = change in z value/ distance between cell centers

The direction is encoded with one of eight values (1,2,4,8,16,32,64,128) to correspond to the orientation of one of the eight cells surrounding the inner grid cell. If the descent to all adjacent cells is the same, the neighborhood is enlarged and the steepest descent found (ESRI, 1994).

Next, the accumulated flow to each cell is calculated using the FLOWACCUMULATION command. Each cell is assigned a value equal to the number of cells that flow into it (Jenson and Dominique, 1988).

b. Next, the ridge lines were delineated by finding all cells with an accumulation less than 1. Cells having a flow accumulation value of zero are local topographic highs and generally correspond to the pattern of ridges (Jenson and Dominique, 1988). Then the ridge lines were grouped into coherent lines while eliminating stray cells.

The REGIONGROUP command was used to first group all cells together into one group of cells. Using this command, all areas with a flow accumulation of zero could be connected together to form coherent ridge lines.

All cells which are "stray" and not part of the main ridge line system are eliminated with the following command (threshold number of cells is 300).

```
ridgegrp1 = select (ridgegrp, 'count > 300')
ridgegrp2 = select (ridgegrp1, 'value > 0')
ridgegrp3 = isnull (ridgegrp2)      GETS RID OF NODATA
ridgegrp4 = con (ridgegrp3 > 0, 1, 0)
ridgegrp5 = setnull (ridgegrp > 1, ridgegrp)
```

c. Next, the distance from the ridge line to each cell is calculated using the EUCDIST command. This command calculates the distance from the center of the source cell to the center of the surrounding cells. The source cells are any cells which make up the ridge line. The Euclidean algorithm calculates, for each cell, the distance to each source cell by calculating the hypotenuse with the x-max and y-max as the other two legs of the triangle (ESRI, 1994).

d. Lastly, the distance to ridge is placed into 20 categories at a 45 meter interval using the slice command. The distance to ridge is reduced to 6 categories by grouping all distances greater than 225 meters into one category, as all distances beyond this point contain no cells affected by landslides.

V. COMPUTATION OF COMPOSITE GRID FOR MAPPING (FAILURE RATE).

To compute the failure rate for each attribute class, the debris slide grid was overlain onto each attribute data layer, and the difference in total number of cells in each class represented the number of cells affected by debris slides. From this information, the failure rate was computed as explained in the text.

Next, the failure rate values in each attribute layer were added together in a simple arithmetic operation as shown:

```
compgrid = slopcat + aspcat + ridgecat + geol + elcat + profg +  
plang
```

The four instability zones were established by computing percentages of the maximum failure rate value.

APPENDIX B - AZIMUTH CALCULATIONS

To compute North-South Vector (degree difference from South, or 180 degrees):

If: aspect < 180 degrees, then $NS = 180 - \text{aspect}$.

aspect > 180 degrees, then $NS = \text{aspect} - 180$.

To compute East-West Vector (degree difference from East, or 090 degrees):

If: aspect < 90 degrees, then $EW = 90 - \text{aspect}$.

270 degrees > aspect > 90 degrees, then $EW = \text{aspect} - 90$.

aspect > 270 degrees, then $EW = 450 - \text{aspect}$.

To compute Dip Vector (degree difference from anti-dip, or 337.5 degrees):

If: aspect < 157.5, then $DIP = \text{aspect} + 22.5$.

337.5 > aspect > 157.5, then $DIP = 337.5 - \text{aspect}$.

aspect > 337.5, then $DIP = \text{aspect} - 337.5$.

VITA

Joseph P. Henderson was born in Birmingham, Alabama on 20 June 1965. He later moved to Maryville, Tennessee where he graduated from Maryville High School in 1983. In June of that year, he entered the United States Military Academy where he received a Bachelor of Science degree in Geography in May 1987.

From 1987 to 1995, he served in a variety of assignments as a commissioned officer in the Aviation Branch of the U.S. Army. Places of duty included the Republic of Korea, Alabama, and Virginia.

In August 1995, he entered the Graduate School of the University of Tennessee. He was awarded the Master of Science degree in Geography in May 1997. After graduation, Captain Henderson will be assigned to the United States Military Academy at West Point, New York, where he will serve as an instructor in the Department of Geography and Environmental Engineering.

He is married to the former Yi Kye Hwa of Chunchon, South Korea. They have two children, Rose Marie and Suzanne Kaylyn.